Journal of Materials Chemistry

Cite this: J. Mater. Chem., 2012, 22, 20649

www.rsc.org/materials

PAPER

Bright, emission tunable fluorescent dyes based on imidazole and π-expanded imidazole†

Kamil Skonieczny,[a] Adina I. Ciuciu,[b] Eva M. Nichols,‡[a] Vincent Hugues,[c] Mireille Blanchard-Desce,*[c] Lucia Flamigni*[b] and Daniel T. Gryko*[ad]

Received 16th June 2012, Accepted 10th August 2012
DOI: 10.1039/c2jm33891b

A diverse set of imidazole- and π-expanded imidazole derivatives displaying excited state intramolecular proton transfer (ESIPT) was designed and synthesized. The effect of structural variation on photophysical properties was studied in detail for nine dyes. The relationship between the structure and photophysical properties was thoroughly elucidated also by comparing with analogues with blocked ESIPT functionality. All but one of the obtained compounds exhibit ESIPT, as demonstrated by large Stokes shifts (6500–15 600 cm^{-1}). The type of π-expansion strongly influences the overall optical phenomena: while typical π-expansion preserves ESIPT activity, the direct fusion of imidazole with a naphthalene unit at positions 4 and 5 results in dyes which do not exhibit ESIPT. The compound possessing an acidic NH group as part of an intramolecular hydrogen bond system has a much higher fluorescence quantum yield and Stokes shift than its analogue bearing an OH group. The occurrence of ESIPT for tosylamide analogues is less affected by the hydrogen-bonding ability of the solvents compared to the unprotected amines. Two-photon absorption cross-sections of the selected derivatives are in the range of 5–100 GM.

Introduction

Imidazole[1] derivatives, pioneered by Debus[2] and Radziszewski,[3] are continuing to attract attention due to their intriguing photophysical properties.[4] While triphenylimidazoles played an important role in the discovery of chemiluminescence,[5] tetraphenylimidazoles have recently attracted significant interest. Ingenious work by Park and co-workers[6] showed that this scaffold, with the proper choice of substituents, can lead to compounds that emit white light through a combination of excited-state intramolecular proton transfer and restricted energy transfer.

Excited-state intramolecular proton transfer (ESIPT)[7] has emerged in recent years as a very interesting phenomenon which can be applied to the design of fluorescent sensors.[8] Typical compounds that display ESIPT, such as benzoxazoles,[9] flavones,[10] 10-hydroxybenzo[*h*]quinoline[11] or imidazo[1,2-*a*]pyridines,[12] possess a large Stokes shift and hence have found applications in laser dyes,[13] fluorescence recording,[14] ultraviolet stabilisers,[15] probes for solvation dynamics,[16] probes for biological environments[17] and recently organic light emitting devices.[6b,18] Excited-state proton transfer is an increasingly important photophysical process in the design of fluorescent probes.[19] Although many functional dyes display ESIPT, only a handful of them are known to simultaneously exhibit a high fluorescence quantum yield. Among those studied extensively is a variety of 2-hydroxyphenylbenzoxazole[9] and 2-hydroxyphenylbenzothiazole derivatives.[20] Very few derivatives and/or analogues of 2-(2-hydroxyphenyl)imidazole have been photophysically studied. Given the promising optical properties of a handful of imidazole derivatives synthesized so far, it is desirable to gain an in-depth knowledge on the structure–property relationship for this group of compounds. In particular, one can envision that π-expansion of multisubstituted imidazoles will significantly alter their optical properties, as is the case for many homoaromatic systems.[21] While phenanthro[9,10-*d*]imidazoles have been previously described,[22a] derivatives possessing a 2-hydroxyphenyl group at position 2 of the imidazole core were studied only recently.[22b] In fluorescence imaging it is desirable to use functional dyes which can be excited using red or NIR light. Given that the majority of ESIPT-active compounds efficiently absorb UV or violet light (hence tissue penetration is rather low and applications in biological imaging are very problematic), we were also interested in studying the two-photon absorption (2PA) cross-section of the selected molecules (which in turn allows for excitation in a biological window) The aim of this study is to explore strategies to

[a]*Institute of Organic Chemistry Polish Academy of Sciences, Kasprzaka 44/52 01-224, Warsaw, Poland. E-mail: dtgryko@icho.edu.pl; Fax: +48 22 632 66 81; Tel: +48 22 343 30 63*
[b]*Istituto per la Sintesi Organica e Fotoreattivita (ISOF), CNR, Via P. Gobetti 101, 40129 Bologna, Italy. E-mail: flamigni@isof.cnr.it; Fax: +39 (0)51 639 98 44; Tel: +39 (0)51 639 98 12*
[c]*Université de Bordeaux, ISM (UMR5255 CNRS), F 33400, Bordeaux, France. E-mail: m.blanchard-desce@ism.u-bordeaux1.fr; Fax: +33 (0)5 40 00 69 94; Tel: +33 (0)5 40 00 67 32*
[d]*Warsaw University of Technology, Noakowskiego 3, 00-664, Warsaw, Poland. Fax: +48 22 628 27 41; Tel: +48 22 234 58 01*
† Electronic supplementary information (ESI) available. See DOI: 10.1039/c2jm33891b
‡ On leave from California Institute of Technology

alter the basic imidazole-based ESIPT system, to obtain a range of derivatives and investigate their fundamental optical properties. This would allow us to address one of the most important challenges regarding ESIPT systems, *i.e.* the wide tunability of chromophore absorption as well as proton transfer emission. Optimization of fluorescence from the keto tautomer remains a challenge in molecular design, with success depending on a more comprehensive understanding of the ESIPT process. The aim of this work is to correlate various structural features with the properties associated with ESIPT and identify promising designs.

Herein we present the synthesis and optical properties of a diverse set of imidazole derivatives and their analogues, combining for the first time a study of ESIPT and 2PA activity.

Results and discussion

Design and synthesis

The occurrence of ESIPT usually leads to a significant decrease in fluorescent quantum yields (ϕ_{fl}) in comparison to analogous non-ESIPT systems.[23] This is mainly due to the competitive internal conversion followed by vibrational relaxation. Park and co-workers showed that tetrasubstituted imidazole derivatives bearing a 2-hydroxyphenyl substituent at position 2 display ESIPT and at the same time possess a fairly high fluorescence quantum yield (0.18).[6]

1,4,5-Triphenyl-2-(2-hydroxyphenyl)imidazole and its analogues absorb around 320 nm and emit light in the range of 460–570 nm. While designing structural variations of this basic chromophore, we kept in mind the two principles: (a) π-expansion of the chromophore should lead to larger ε and may result in higher σ_2; (b) both linear and 2PA properties will depend on the type of π-expansion, thus suggesting that various types of 1,2-diketones should be utilized. We also would like to include NH hydrogen bond donors in addition to commonly used phenolic OH groups. Keeping in mind the above considerations, a small library of nine derivatives was designed. We envisioned that all ESIPT-compounds, as well as analogs with blocked ability to form hydrogen bonds, could be synthesized *via* the Debus–Radziszewski method. Among various possibilities to expand the imidazole chromophore, conceptually the easiest is to start from 1,10-phenantroquinone (**1**) (Scheme 1). Condensation of diketone quinone **1** with aniline (**2**) or *p*-toluidine (**3**) and salicylaldehyde gave a mixture of π-expanded imidazole **7** and known[24] π-expanded oxazole **8** in moderate yields. The concomitant formation of oxazole derivatives is in agreement with the well-known Japp reaction for benzoxazole synthesis.[25] The model compounds **6** and **9** were synthesized either *via* direct condensation starting from *o*-anisaldehyde or *via* methylation of hydroxyl-derivative **8** (Scheme 1). Two analogous compounds **11** and **12** were synthesized from quinone **10** (Scheme 2). They differ from **6** and **7** in that they possess two additional pyridine-type nitrogens which decrease electron density in the heterocyclic system, allowing at the same time to build complexes of $Ru(phen)_3$ type.

It is known that rylene type π-expansion gives a significantly larger bathochromic shift in absorption compared to the addition of a naphthalene unit in an anthracene-like fashion.[26] Along these lines, we designed and synthesized expanded imidazoles **14** and **15** starting from acenaphthoquinone (**13**) (Scheme 3). A moderate yield of the Debus–Radziszewski condensation using ketone **13** is expected given previous literature data.[27] As previously reported the main product of this reaction is acenaphtho

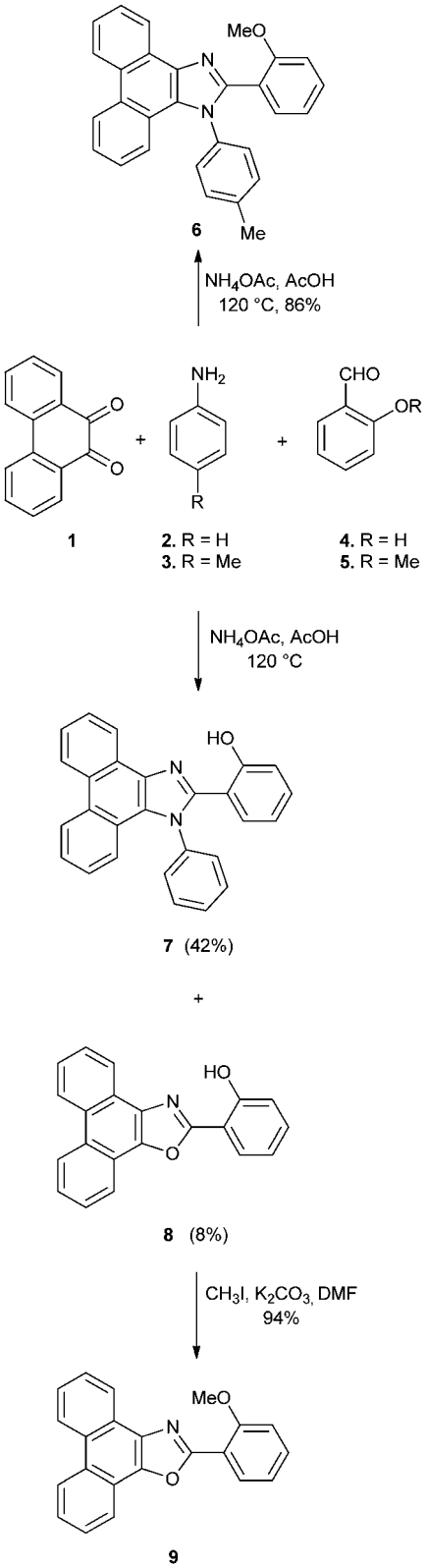

Scheme 1

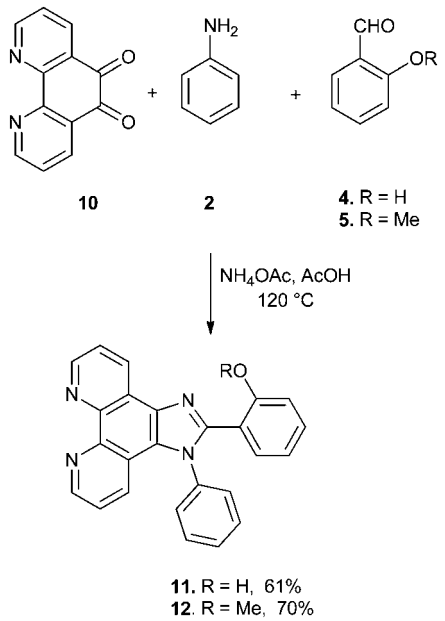

Scheme 2

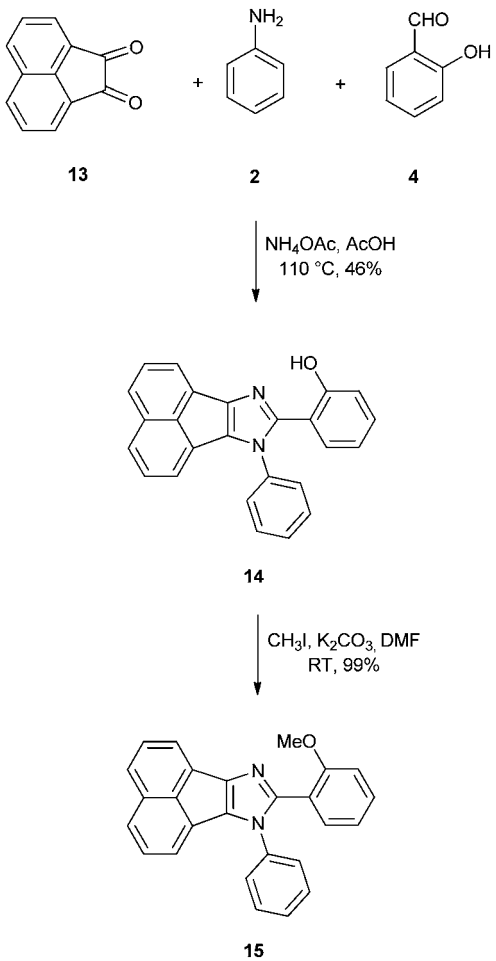

Scheme 3

[1′,2′:4,5]imidazo[2,1-*a*]benzo[*de*]isoquinolin-14-one.[28] Due to the significant difference in R_f it was easily separated from the desired compound **14**.

A second group of compounds was designed to study the N–H–N hydrogen bond system. We were curious to investigate the

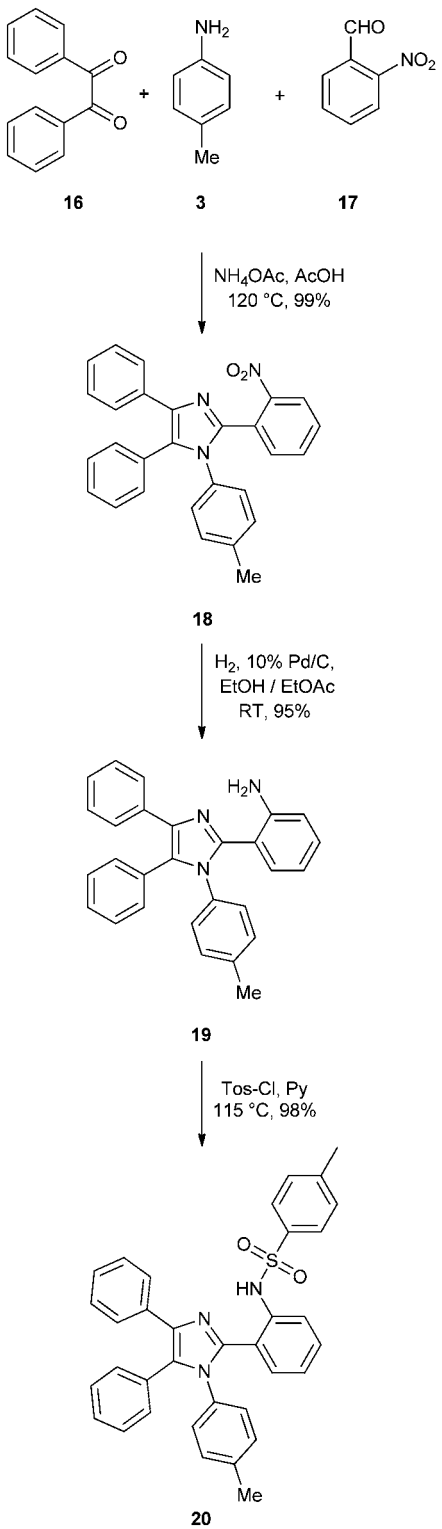

Scheme 4

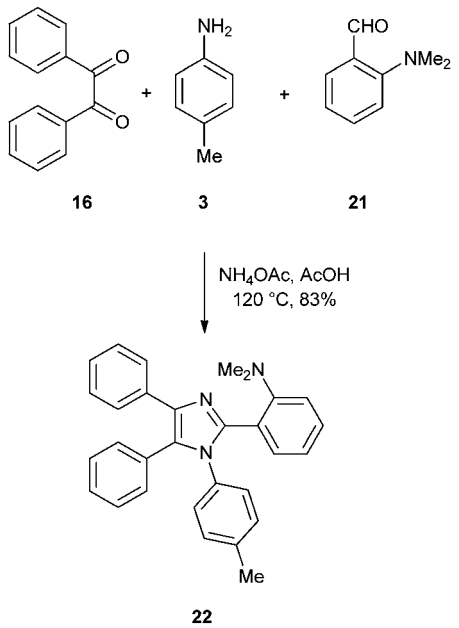

Scheme 5

difference in optical properties of these compounds as a function of acidity of the N–H bond. Five compounds (**19**, **20**, **24**, **25** and **27**) were designed and synthesized. The key compounds **20** and **25** possess an *N*-tosylamino group at the *ortho* position of the phenyl ring. Since the corresponding aldehyde is not commercially available, our syntheses started from 2-nitrobenzaldehyde **17** (Schemes 4 and 6).

The synthesized imidazole **18** was easily reduced to compound **19** and tosylated under classical conditions to obtain the target derivative **20** in a 92% overall yield. In order to compare optical properties of imidazole **20** with amine **19** and the model compound lacking ESIPT activity, we synthesized derivative **22** from the corresponding aldehyde **21** [29] (Scheme 5).

Synthesis of the fused analogue of compound **20** was realized using the same strategy starting from 2-nitrobenzaldehyde (**17**) and 1,10-phenantroquinone (**1**) in an overall yield of 84% (Scheme 6). Imidazole **27** was synthesized starting from aldehyde **26** (Scheme 7). Given the moderate acidity of the N–H bond, it was expected that this arrangement would lead to a weak hydrogen bond. This type of structural variation is interesting since it results in a different geometry of the intramolecular hydrogen bond.

Linear optical properties

The ESIPT process is very complex and its efficiency is affected by internal (*e.g.* substitution pattern) or external parameters (*e.g.* solvent). In order to ascertain the ESIPT properties of the new compounds, we determined their basic spectroscopic properties and compared them to those of non-ESIPT models in solvents of different dielectric constants and proticities, namely toluene (Tol), dichloromethane (DCM) and methanol (MeOH). Molar absorption coefficients and related absorption maxima, emission maxima, Stokes shifts, and luminescence quantum yields are reported in Table 1. Where appropriate, two separate lines for the enol and keto forms are reported.

Compound **8**, the only benzoxazole of the series, could in principle exist, in analogy to similar benzoxazoles, in the two different planar conformers *syn* and *anti* enols in equilibrium in the ground state. In addition, in H-bonding solvents a third non planar rotamer, referred to as *open* or *solvated*, where the phenoxy group is H-bonded to a solvent molecule, can be present

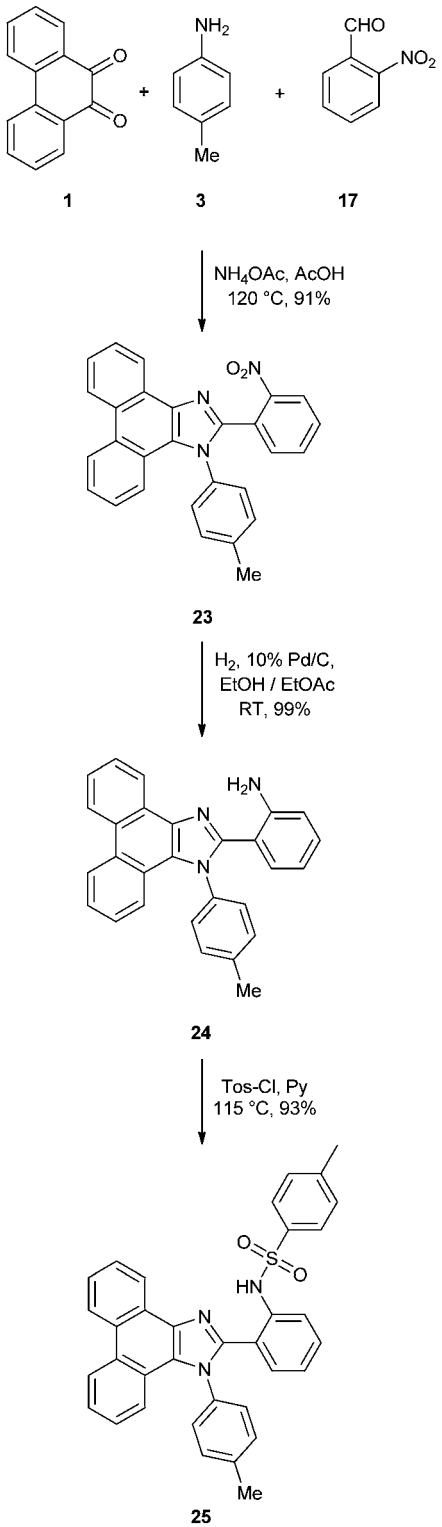

Scheme 6

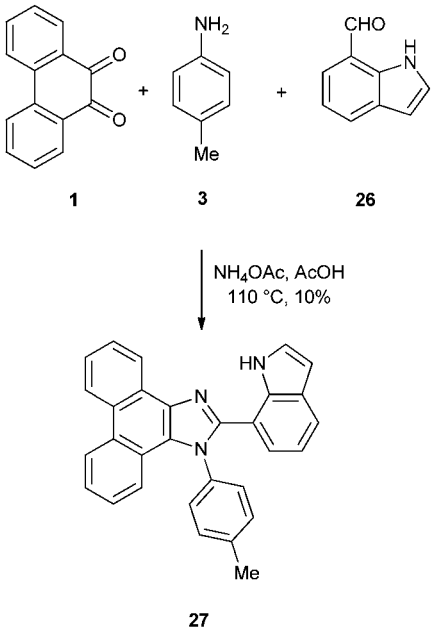

Scheme 7

(Fig. 1).[30] The *syn* form, due to favorable electronic and structural properties, exhibit ESIPT whereas the *anti* form does not lead to ESIPT because of unfavorable thermodynamic parameters. In apolar or low polarity solvents the *syn* form prevails due to the relatively stronger H-bond with the benzoxazole N rather than with O. In polar solvents, on the contrary, the perpendicular *open* form prevails but still some *anti* and *syn* forms are present in low concentration. Therefore, it has been shown that in simple 2-hydroxyphenylbenzoxazole (HBO) in apolar solvent only the keto form emission prevails, that in polar solvents the enol form appears, whereas in protic methanol both forms are present.[30] This phenomenology is actually affected by the substitution pattern, and a different distribution of the emission of the keto and enol forms has been found in hydroxynaphthyl derivatives, for example.[31] The main reason for the different behavior depends on the energy barrier between the *syn* and *anti* forms in the enol ground state whose height is strongly affected by substitution.

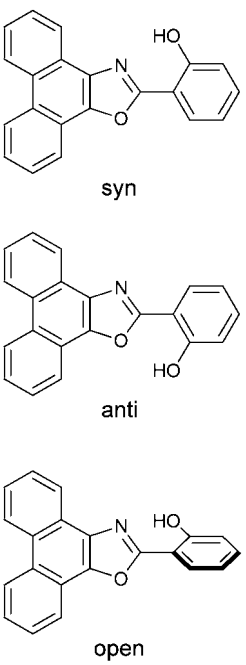

Fig. 1 Possible conformers of compound **8**.

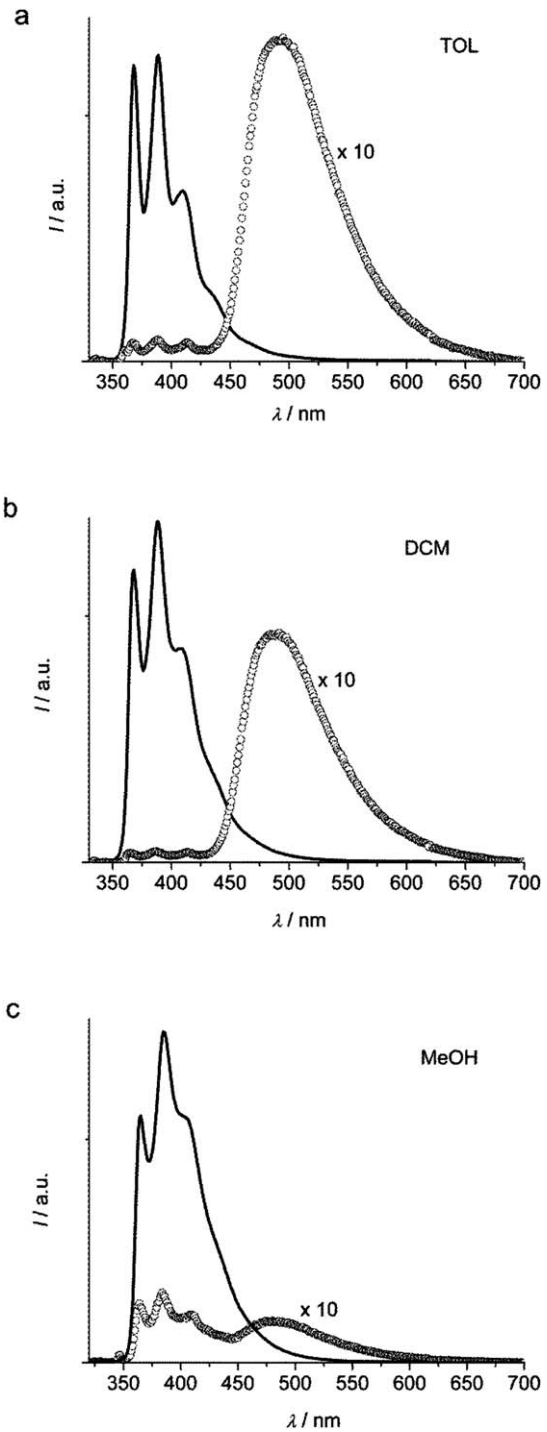

Fig. 2 Fluorescence from optically matched solutions of **9** (line) and **8** (scattered) in Tol, DCM and MeOH. The signal from **8** is multiplied by 10. The excitation wavelength is 325 nm in Tol, 327 nm in DCM and 315 nm in MeOH.

Table 1 Spectroscopic properties of compounds **9**, **8**, **6**, **7**, **12**, **11**, **15**, **14**, **22**, **19**, **20**, **24**, **25** and **27** in toluene, dichloromethane and methanol. Reference models are in italics

		Toluene				*Dichloromethane*				Methanol			
		ε_{max}/M^{-1} cm^{-1} (λ_{max}/nm)	λ_{em}/nm	$\Delta\nu_{ss}$/cm^{-1}	ϕ_{fl}[a]	*ε_{max}/M^{-1} cm^{-1} (λ_{max}/nm)*	*λ_{em}/nm*	*$\Delta\nu_{ss}$/cm^{-1}*	*ϕ_{fl}[a]*	ε_{max}/M^{-1} cm^{-1} (λ_{max}/nm)	λ_{em}/nm	$\Delta\nu_{ss}$/cm^{-1}	ϕ_{fl}[a]
9		20 200 (329); 13 900 (364)	368; 389; 410	300	0.53	*48 200 (259); 17 800 (329); 12 000 (363)*	*368; 388; 409*	*370*	*0.58*	58 000 (256); 20 400 (325); 12 500 (360)	365; 385; 405	380	0.602
8	E	24 800 (344); 28 200 (364)	367; 389; 413	230	0.003	*47 100 (259); 22 200 (343);*	*365; 387; 414*	*230*	*0.001*	41 800 (257); 19 100 (340);	364; 384; 410	305	0.009
	K		495	7270	0.111	*24 800 (362)*	*492*	*7300*	*0.073*	21 300 (360)	480	6940	0.013
6		14 000 (309); 3600 (342); 3800 (359)	371; 384	900	0.284	*70 400 (260); 20 800 (285); 12 600 (307); 3000 (340); 3200 (357)*	*370; 385*	*980*	*0.294*	102 300 (256); 27 500 (283); 16 800 (303); 4000 (336); 4200 (353)	363; 378	780	0.271
7	E	24 800 (335);	369; 383	300	<0.001	*56 900 (263);*	*370; 390*	*440*	*<0.001*	69 600 (258);	365; 379	303	0.005
	K	21 300 (347); 23 000 (365)	478	6480	0.191	*24 100 (333); 19 700 (346); 21 100 (364)*	*473*	*6330*	*0.144*	15 900 (330); 12 800 (343); 13 000 (361)	473	6560	0.018
12		10 700 (317); 2000 (363)	377 (sh); 396; 418 (sh)	1020	0.064	*39 800 (256); 30 800 (285); 1300 (357)*	*405*	*3320*	*0.075*	45 300 (254); 32 900 (284); 1300 (357)	429	4700	0.040
11	E	25 600 (334)	379; 400	3550	<0.001	*40 500 (276);*	*398*	*4995*	*0.002*	40 100 (254);	423	6850	0.002
	K		484	9280	0.125	*25 300 (332)*	*484*	*9460*	*0.073*	35 600 (277); 12 900 (328)			
15[a]		19 500 (312); 900 (428)	382; 571	5870; 5851	0.010	*19 300 (310); 800 (424)*	*388; 576*	*6480; 6223*	*0.009*	19 300 (306); 800 (412)	387; 568	6840; 6670	0.007
14		36 500 (327); 1800 (430)	575	5860	0.009	*36 000 (325); 1500 (428)*	*590*	*6415*	*0.006*	26 600 (321); 1300 (420)	583	6660	0.005
22		>20 000 (<275)	422	>12 700	0.275	*24 000 (261)*	*424*	*14 730*	*0.278*	24 600 (255)	430	15 960	0.275
19	E	17 600 (282);	398	5360	0.009	*17 000 (282);*	*397*	*5300*	*0.007*	17 600 (275)	407	11 790	0.057
	K	12 300 (328)	572	13 000	0.004	*10 100 (328)*	*562*	*12 690*	*0.002*		—	—	—
20	E	18 000 (300)	375	6670	0.004	*17 900 (287)*	*378*	*8390*	*0.004*	18 100 (275)	379	9980	0.004
	K		499	13 290	0.396		*484*	*14 180*	*0.362*		482	15 620	0.201
24	E	14 000 (311);	396; 410	2290	0.173	*63 200 (260);*	*397; 410*	*2511*	*0.128*	76 300 (257);	415	4300	0.283
	K	12 800 (342); 10 700 (363)	—	—	—	*14 500 (309); 11 800 (341); 9700 (361)*	—	—	—	14 200 (304); 7100 (335); 5900 (352)	—	—	—
25	E	18 500 (328); 14 300 (344);	365; 383; 408	300	0.007	*57 600 (262); 18 700 (327);*	*368; 384; 407*	*600*	*0.011*	52 700 (259); 12 900 (324);	364; 381; 404	550	0.015
	K	12 700 (361)	506	7950	0.468	*13 900 (343); 12 600 (360)*	*495*	*7600*	*0.515*	9200 (341); 8500 (357)	497	7900	0.171
27	E	18 900 (342); 18 900 (354);	377; 398; 421	280	0.170	*32 900 (265); 16 700 (340);*	*377; 398; 420*	*360*	*0.234*	45 900 (257); 11 900 (336),	373; 394; 415	290	0.215
	K	20 900 (373)	566	9140	0.015	*16 200 (353); 17 400 (372)*	*556*	*8900*	*0.011*	10 400 (350); 8600 (369)	565	9400	0.005

[a] The emission quantum yield is calculated by adding the area of the 382–387 nm band to that of the 568–576 nm band.

Going back to the case of **8** in Tol, this is characterized by an enol form with a structured emission band with maxima at 367, 389, and 413 nm, well reproducing the non-ESIPT model **9** with maxima at 368, 389 and 410 nm (Fig. 2).

The luminescence however is greatly quenched, to less than 1% that of the model (Table 1). The keto form with a maximum at 495 nm has a yield of 0.111. In DCM, the luminescence properties are very similar to Tol – a very low emission yield of the enol form, and emission from the keto form with $\phi_{fl} = 0.073$. In MeOH, however, the ratio between enol and keto form changes, and the enol emission yield grows above 1% of the model emission whereas the luminescence of the keto form drops to an emission quantum yield of 0.013.

This is in agreement with the fact that the *anti* form is more stable in polar solvents, as formerly observed.[24] The present case seems to have more similarities with that of similar 2-hydroxynaphtyl derivatives, where the enol form could be observed also in benzene, than with that of HBO. Very likely, also in this case the barrier between *syn* and *anti* conformers is rather low. The replacement of the oxygen atom with the NC_6H_5 group leads to π-expanded imidazole **7**. This alteration changes the central unit to the one which is less electron deficient.

A single isomer is possible; in Tol the enolic form has bands at 369 and 383, very similar to the spectrum of model **6**. The luminescence of this form is however almost completely quenched in favor of the appearance of the keto form emission at 478 nm, with a ϕ_{fl} of almost 0.2. The results in DCM are rather similar, with a slightly lower emission quantum yield of the keto form of 0.144, and a 5 nm hypsochromically shifted maximum. In the protic solvent (MeOH) the luminescence of the keto form diminishes by a factor of almost 10 compared to Tol whereas the emission of the enol form appears at 365 and 379 nm, in good agreement with that of model **6** (Fig. 3). Whereas in non-protic solvents the ground state configuration with a pre-formed H bond between hydroxyl H and the N3 of the imidazole favors ESIPT, in MeOH intermolecular H-bonding with the solvent competes with the intramolecular one, limiting the ESIPT process only to the intramolecularly bound structures.

Because the effective conjugation length is affected by the planarity of the molecule, phenanthro[9,10-*d*]imidazole **7** when compared to 1,4,5-triphenyl-2-(2-hydroxyphenyl)imidazole[6a] reveals a significant bathochromic shift of absorption (~45 nm). The extended conjugation length however has only an indirect and limited effect on the stabilization of the keto excited state, resulting in a small change in the emission (~10 nm). Needless to say the Stokes shift ($\Delta\nu_{ss}$) decreases from 11 000 cm^{-1} to ~6500 cm^{-1}. At the same time ϕ_{fl} remains on the same level. The direct comparison of optical properties of compound **7** with analogues studied by Park *et al.* as well as with other tri- and tetrasubstituted imidazole derivatives[32–35] reveals similar trends.

The phenanthroline derivative **11** displays in Tol a luminescence mainly of keto type, with a maximum at 484 nm and an emission quantum yield of 0.125, twice the one of the enol luminescence of the reference model **12** (Fig. 4). In Tol the enol luminescence is reduced to an extremely low value, which increases slightly in DCM. Conversely in DCM the luminescence of the keto form decreases to about half with respect to that in Tol. In MeOH model **12** displays a different spectrum, bathochromically shifted and with a reduced luminescence quantum yield with respect to the former less polar, aprotic solvents. This seems to indicate that in the non-ESIPT model **12** in protic polar solvents, the excited state is different than in less polar solvents. Accordingly, also in the ESIPT compound **11** the luminescence in the higher energy side is bathochromically shifted whereas the keto form emission disappears. We ascribe this behavior in the protic polar solvent either to the stabilization of a CT state, which becomes the emitting one or, less likely, to the emission from a differently protonated form of phenanthroline derivative. When compared to compound **7**, dye **11** displays a significantly higher Stokes shift in non-polar solvents (9300 *vs.* 6500 cm^{-1}) and lower emission quantum yield (Table 1). For both dyes **6** and **12** absorption maximum is basically solvent-independent and the presence of two nitrogen atoms has a negligible effect on the spectrum. As for dye **12** this is in contrast with results published for 1,2-diaryl-phenantrolinoimidazoles with 4-substituted aryl groups, which display a slight but noticeable bathochromic shift of absorption while moving to polar solvents.[36a,b] The situation is entirely different for emission. While emission maximum of model compound **6** is almost solvent-independent, for dye **12** it does bathochromically shift with increasing solvent polarity. The fluorescence quantum yield of dye **12** is also decreased when compared to analogue **6** (only 0.04–0.075 depending on the solvent). This cannot however be simply explained by the presence of two pyridine-type nitrogen atoms, since fluorescence quantum yields reported for analogous compounds lacking steric hindrance imparted by the 2-methoxy group are around 0.4.[36a,b] Crystallographic studies show that the mean plane angle between the imidazole ring makes a dihedral angle of 56° with a phenyl ring attached to the C(2) carbon.[36a,b] The presence of an additional substituent at position 2 imparts steric hindrance which in turn can probably increase this dihedral angle, decreasing effective conjugation in the ground state. In spite of that we did not observe a notable hypsochromic shift of absorption of compounds **6** and **12** compared to non-hindered analogues.[36c]

Altering the mode of π-expansion resulted in a complete change in the optical properties of the resulting dyes **14** and **15**. Compound **14** has luminescence properties which are hardly distinguishable from those of the non-ESIPT model **15** (Fig. 5). The only difference is the presence in model **15** of a weak emission around 385 nm, absent in **14**. Both model and ESIPT display a strong Stokes-shifted broad band, bathochromically shifted in **14** with respect to the model by 5 nm in non-polar Tol and by *ca.* 15 nm in DCM and MeOH. The luminescence yield of the Stokes-shifted band in **14** ($\phi_{fl} \leq 10^{-2}$) is lower with respect to model **15** by 10% in Tol and by almost 30% in DCM and MeOH. The same behavior is obtained with excitation on the visible band at 580 nm.

The plausible rationale behind these data is that the energy difference between S1 levels of the keto and enol tautomers is small and this precludes ESIPT to occur for thermodynamic reasons (in analogy to a 10-hydroxy-1-azaperylene scaffold).[37] Rather large Stokes shifts for both **14** and **15** suggest an important geometry and/or electron-distribution rearrangement in the S1 excited state. The comparison of two types of π-expansion (**14** *vs.* **7**) reveals a significant difference. Dye **14** has bathochromically shifted (although weak) absorption toward the visible region, relatively high Stokes shift and ϕ_{fl} is only 1%. It is noteworthy to mention that this is the first photophysical investigation of π-expanded imidazoles of this type.

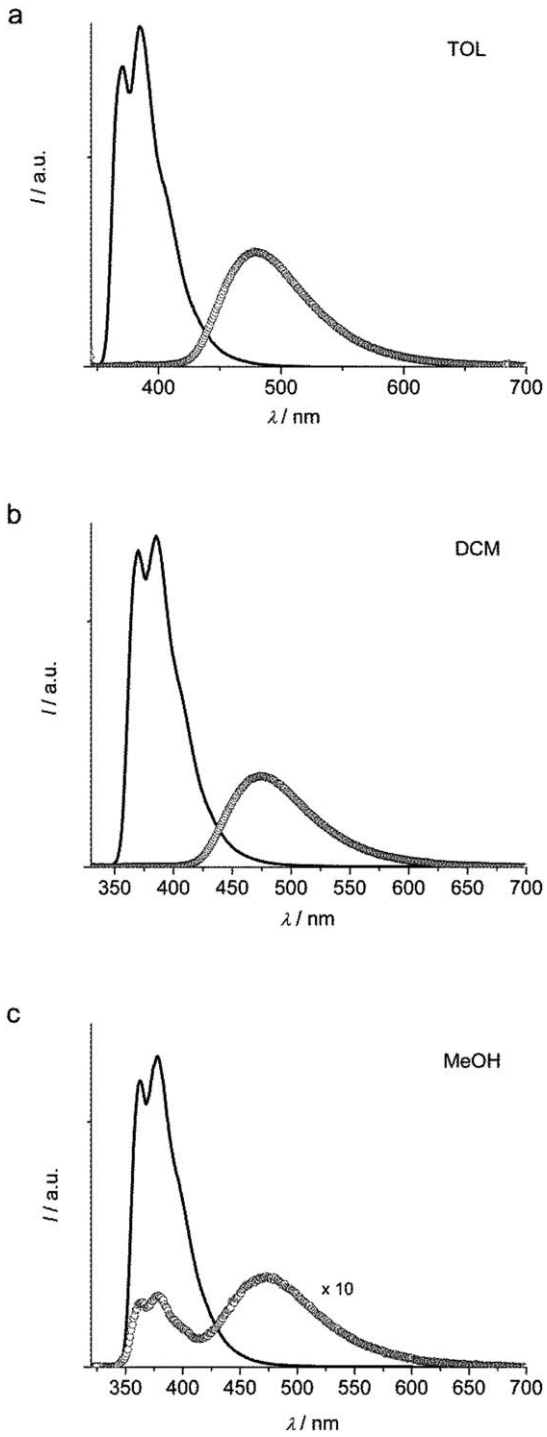

Fig. 3 Fluorescence from optically matched solutions of **6** (line) and **7** (scattered) in Tol, DCM and MeOH. The signal from **7** in MeOH is multiplied by 10. The excitation wavelength is 343 nm in Tol, 324 nm in DCM and 315 nm in MeOH.

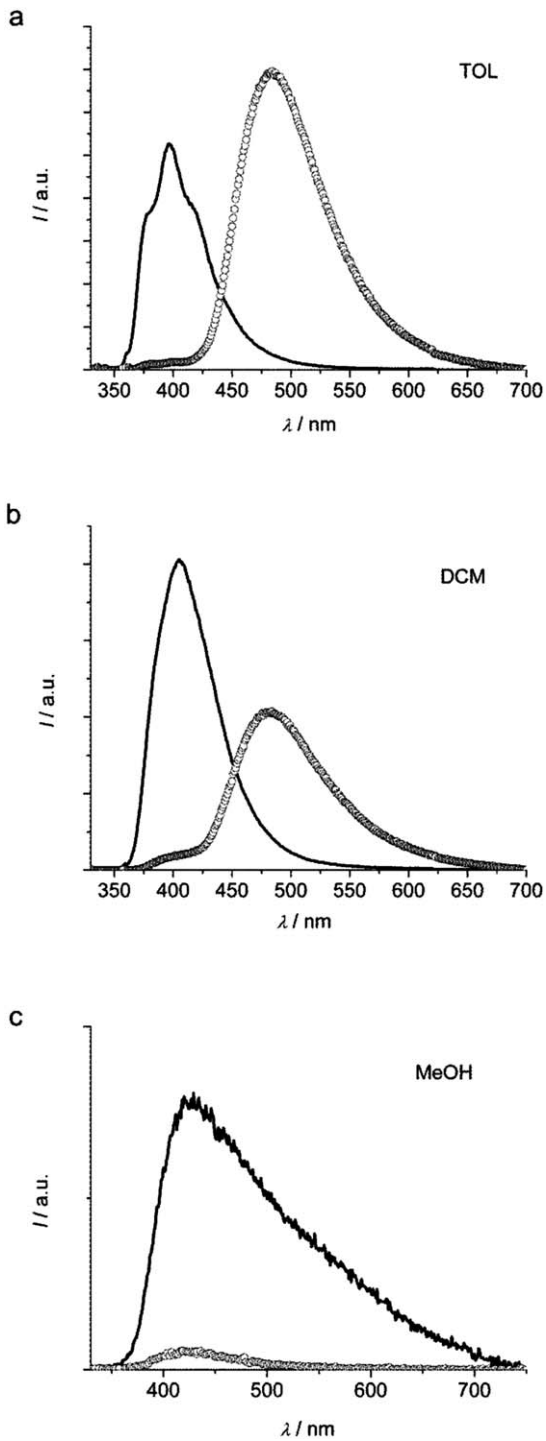

Fig. 4 Fluorescence from optically matched solutions of **12** (line) and **11** (scattered) in Tol, DCM and MeOH. The excitation wavelength is 325 nm in Tol, 324 nm in DCM and 325 nm in MeOH.

In the second part of photophysical studies we focused on compounds bearing NH group as a donor in a hydrogen bond. The properties of **19** and **20** will be discussed relative to the non-ESIPT model **22**. The luminescence of model **22** is rather atypical for an enol luminescence, generally structured, and points to a mixing with a low energy charge transfer (CT) state. The presence of such a low energy state is compatible with the presence of the electron rich amino group in the model which might act as an electron donor toward the imidazole moiety. Interestingly the effect of the NMe_2 group at position 2 of the phenyl ring is different than for an analogous tetraphenylimidazole possessing a 4-*N*,*N*-dimethylaminophenyl substituent $\phi_{fl} = 0.31$.[38] Although ϕ_{fl} of compound **22** is almost the same (0.28) in comparison with

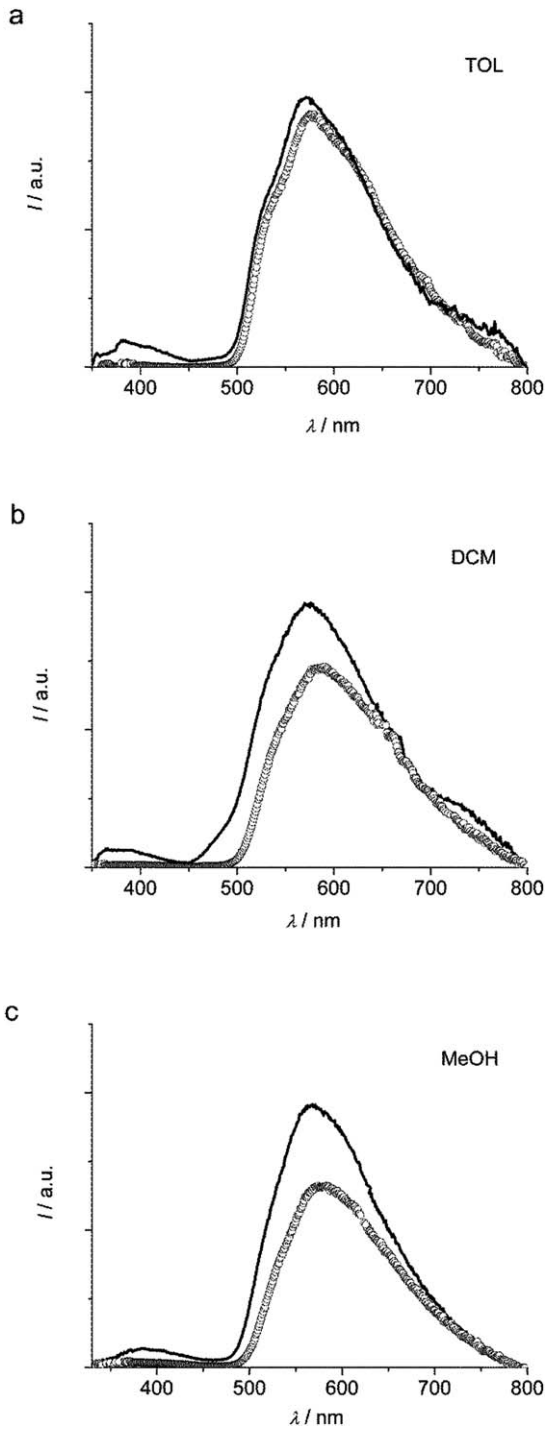

Fig. 5 Fluorescence from optically matched solutions of **15** (line) and **14** (scattered) in Tol, DCM and MeOH. The excitation wavelength is 342 nm in Tol, 326 nm in DCM and 326 nm in MeOH.

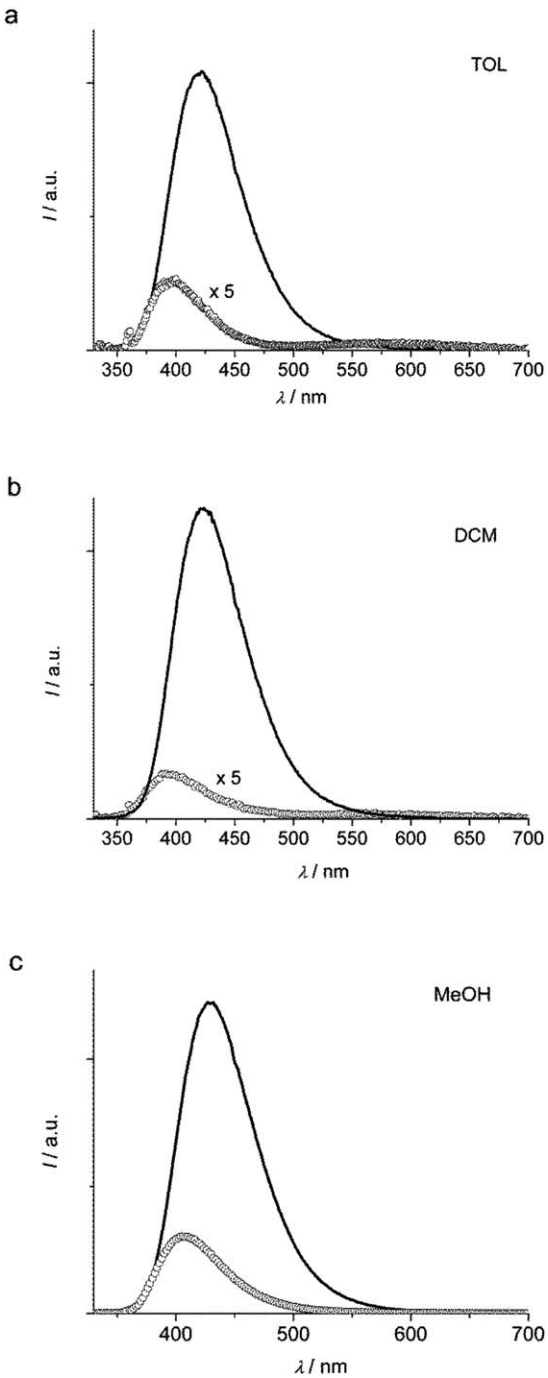

Fig. 6 Fluorescence from optically matched solutions of **22** (line) and **19** (scattered) in Tol, DCM and MeOH. The signal from **19** in Tol and DCM is multiplied by 5. The excitation wavelength is 325 nm in Tol, in DCM and in MeOH.

imidazole bearing 4-*N*,*N*-dimethylaminophenyl group, the fluorescence maximum is strongly red shifted and the absorption maximum is strongly blue shifted. As a result the Stokes shift is significantly higher ($\sim$16 000 cm^{-1} *vs.* 8500 cm^{-1}). The relative blue shift of absorption in compound **22** originates from steric hindrance induced by the presence of the NMe_2 group at position two of the phenyl ring decreasing the effective interaction between this ring and the imidazole core in the ground state.

In **19** the luminescence is shifted to higher energies with respect to model **22**, which is compatible with a less electron rich NH unit which destabilizes the CT state. However, the "enol" luminescence is generated also in this case from a state with a sizeable CT component. Accordingly, the fluorescence band shifts to a lower energy in the more polar solvent (MeOH) which stabilizes CT. The luminescence maximum shifts in fact from 398 nm in TOL to 407 nm in MeOH (Fig. 6). Whereas in Tol and DCM

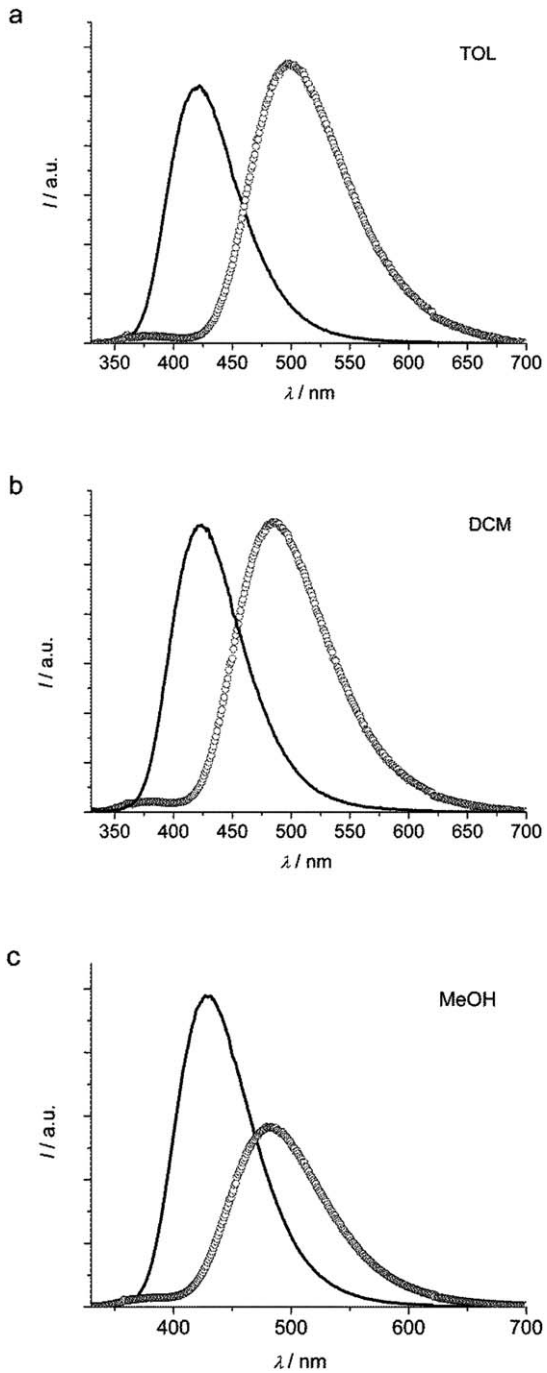

Fig. 7 Fluorescence from optically matched solutions of **22** (line) and **20** (scattered) in Tol, DCM and MeOH. The excitation wavelength is 325 nm in Tol, 325 nm in DCM and 330 nm in MeOH.

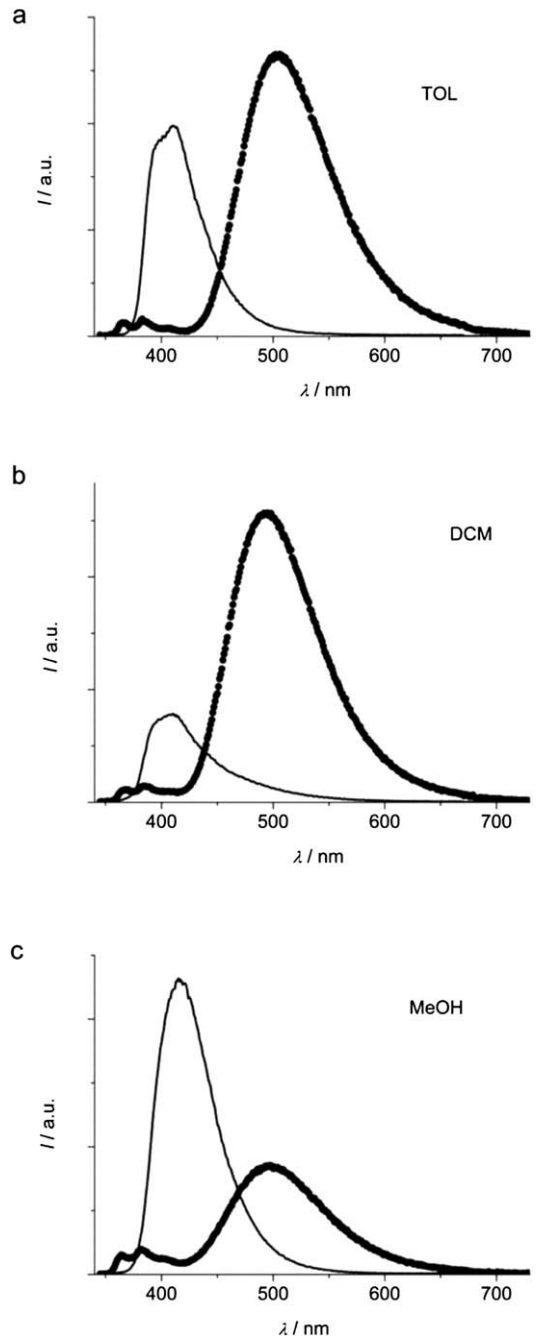

Fig. 8 Fluorescence from optically matched solutions of **24** (line) and **25** (scattered) in Tol, DCM and MeOH. The excitation wavelength is 343 nm in Tol, DCM and MeOH.

some keto forms can be detected (though to an extremely low extent, $\phi_{fl} < 10^{-2}$) it disappears completely in MeOH, where the emission is only from the enol/CT state. Proton coupled electron transfer (PCET) reactions associated with electronically excited states is an interesting class of reactions[39] and the present case seems to belong to this class.

The introduction of the electron-withdrawing tosyl group in **20** leads to a completely different behavior (Fig. 7). The NH group is now less electron rich due to the inductive effect of the substituent, therefore a low energy CT excited state involving the imidazole unit is no longer possible. The difference in peak wavelength between absorption and emission as large as 15 000 cm^{-1} unambiguously supports the occurrence of ESIPT, forming a proton-transfer tautomer adiabatically in the excited state.

In Tol a strongly quenched enol fluorescence at 375 nm with $\phi_{fl} = 0.004$ is observed, but an intense keto luminescence with ϕ_{fl} of almost 0.4 is registered at 499 nm. In DCM the behavior is similar, with a similarly low enol fluorescence at 378 nm and a slightly hypsochromically shifted keto luminescence at 484 nm

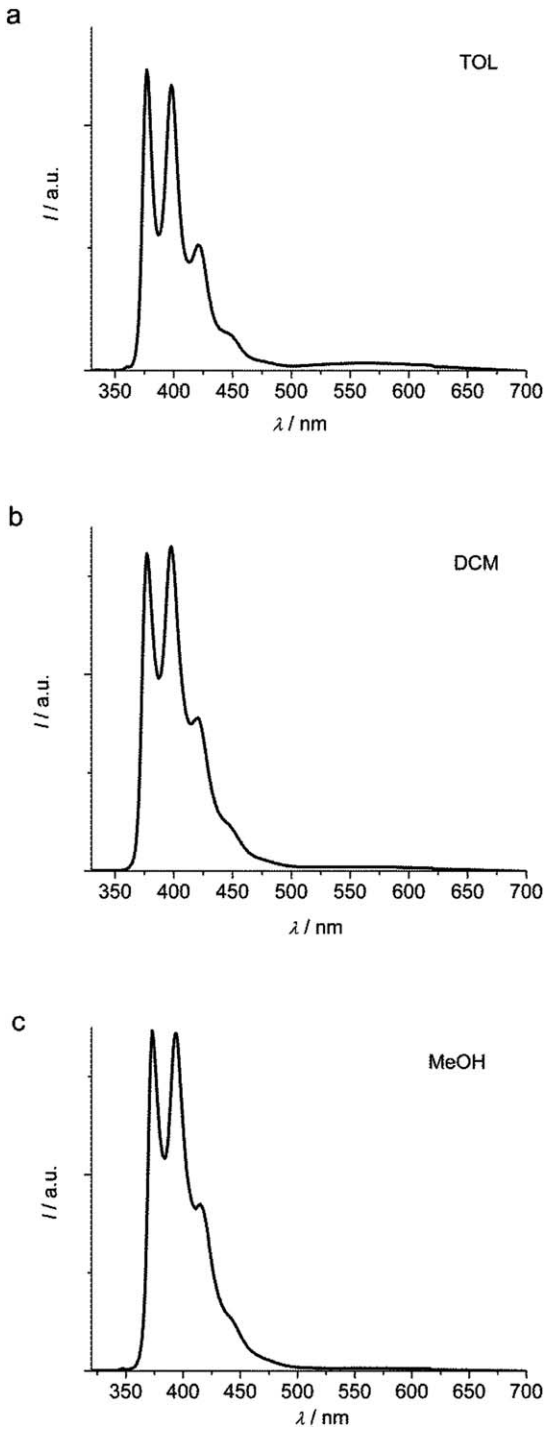

Fig. 9 Fluorescence from solutions of **27** in Tol, DCM and MeOH. The excitation wavelength is 325 nm in Tol, 327 nm in DCM and 315 nm in MeOH.

with an almost identical emission quantum yield to that of Tol. In MeOH the protic solvent competes with the intramolecular H-bond formation decreasing the ESIPT efficiency. As a consequence the keto fluorescence at 482 nm is decreased to $\phi_{fl} = 0.201$ in MeOH whereas the enol luminescence is almost constant with respect to Tol and DCM.

Dyes **24** and **25** are the equivalents of compounds **19** and **20** respectively, but with the more extended aromatic unit (phenanthrene). Compound **24** shows a moderately intense, enol like emission in Tol and DCM (ϕ_{fl} *ca.* 0.15) but with a slightly higher Stokes-shifted emission than expected (Fig. 8 and Table 1). This indicates some charge transfer characters in the excited state, though much lower than the one detected in **19** (where it is visible both from the broad spectral shape and from the larger Stokes shifted emission). Only in MeOH the structureless spectral shape and the higher Stokes shift of **24** are more clearly indicative of a charge transfer emitting excited state. In this solvent, the luminescence yield is rather intense (~0.3). In comparison with **19**, **24** has a much higher fluorescence intensity and does not display the minimal formation of a keto form, which was on the contrary detectable in **19**. Obviously, in the present case there is no sufficient driving force for proton transfer to occur in the excited state.

Upon introduction of the electron-withdrawing tosyl group in **25**, which renders the NH group less electron rich, the enolic excited state loses its charge transfer character and displays a structured emission. As in the case of **20**, the keto form is efficiently formed, displaying ϕ_{fl} on the order of 0.5 in non-polar and moderately polar solvents. Even in MeOH, where the competition with the solvent generally precludes or disfavors ESIPT, the keto form has a high yield of formation, as testified by the still moderately high emission yield of the keto form, on the order of 0.2. The phenomenology in both compounds **24** and **25** can be interpreted along the same lines as **19** and **20**.

As described by Fahrni and co-workers for 2-(2′-tosylaminophenyl)benzimidazoles, the *cis*-rotamer is thermodynamically substantially favored over the *trans*-rotamer.[40] As a result the ground-state equilibrium of that molecule is dominated by a single species, and the ESIPT process is essentially unaffected by the nature of the solvent.[40] In the case of tosylamides **20** and **25** ESIPT is more affected by solvent properties than in the corresponding benzimidazole case[40] but much less than for phenols **7** and **11**. Notably, both derivatives **20** and **25** exhibit mostly keto-emission, indicating that formation of ESIPT tautomer is very efficient and neither compromised through solvent–solute hydrogen-bonding interactions,[41] solvent-polarization-induced barriers,[42] or ground-state stabilization of tautomer that cannot undergo ESIPT.[43]

Compound **27** displays a spectrum clearly ascribable to the enolic form, with a structured emission with maxima at 377, 398 and 421 nm in Tol and an emission quantum yield of 0.17. A very weak emission of a keto form with maximum at 566 nm and $\phi_{fl} = 0.015$ can be detected in Tol (Fig. 9). The emission quantum yield of the enolic form increases in polar solvents whereas that of the keto form decreases. In this molecule ESIPT appears to be ineffective very likely for the low acidity of the indolic proton.

Non-linear optical properties

Two-photon absorption measurements of selected ESIPT chromophores (**7**, **8**, **11**, **19** and **20**) were performed using the two-photon excited fluorescence (TPEF) method (Table 2). Unfortunately, measurements of compounds **11** and **20** were not possible as they did not give a reliable TPEF signal (the fluorescence quantum yield of **11** is too low and the 2PA of **20** in the 700–900 nm region is too low due to its blue-shifted absorption).

Table 2 Two-photon absorption (2PA) cross-section of compounds **7**, **8**, **11**, **19** and **20**

Compound	Solvent	λ_{2PA}^{max1} (nm)	σ_2^{max1} (GM)
7	CH_3CN	<700	>18
8	$CHCl_3$	710	5
11	CH_3CN	—	—
19	$CHCl_3$	<700	>95
20	$CHCl_3$	—	—

Among all compounds studied, dye **19** gave the highest 2PA cross-section value (about 100 GM), while compounds **7** and **8** possess lower values (~5 to 20 GM). Interestingly, we found a five-fold increase of 2PA at 700 nm on going from π-expanded oxazole **8** to π-expanded imidazole **7**. However, since the oxazole derivative has a lower quantum yield, this results in similar two-photon brightness. Furthermore, replacing OH with NH_2 (a stronger donor) leads to much larger 2PA in the 700–800 nm region (although it is hypsochromically shifted and fluorescence blue-shifted).

Conclusions

In conclusion, we report new functional dyes combining record Stokes shifts (15 000 cm^{-1}) with good fluorescence quantum yields and reasonable ε values. We also discovered that specific π-expansion of imidazole derivatives leads to an ESIPT-silent system that still possesses a large Stokes shift. Another non-ESIPT architecture which leads to a similar effect is 1,4,5-triphenyl-2-(2′-dimethylaminophenyl)imidazole. The other notable findings are as follows: (a) in most cases, π-expansion of the chromophore leads to compounds that display an excited state intramolecular proton transfer, as evidenced by a large Stokes shift. A detailed study of the optical properties of the products and their ESIPT-blocked models allowed us to observe that substitution of OH with H–N–Tos led to an increase in the Stokes shift while hypsochromically shifting the absorption band. We found that chemical modifications resulted in significantly altered spectroscopic properties (*i.e.*, red-shifted absorption and emission spectra) relative to the parent 1,4,5-triphenyl-2-(2-hydroxyphenyl)imidazole. The key difference between dyes possessing the OH group *versus* the NHT group is that for the latter ones the keto state is achievable even in MeOH. These results are not only of theoretical significance in that they provide new insight into factors influencing the ESIPT phenomenon, but they may also open doors to practical applications in biological imaging.

Experimental part

Synthesis

All chemicals were used as received unless otherwise noted. Reagent grade solvents (CH_2Cl_2, hexanes) were distilled prior to use. All reported NMR spectra were recorded on 500 MHz and 600 MHz spectrometers. UV-vis absorption and fluorescent spectra were recorded in acetonitrile. Chromatography was performed on silica (200–400 mesh). Mass spectra were obtained *via* EI-MS. Aldehyde **21** (ref. 29) and diketone **10** (ref. 44) were prepared according to the literature procedures.

General procedure for 1. To a solution of aromatic aldehyde (1 eq.) and aromatic amine (1.5 eq.) in glacial acetic acid, α-diketone (1 eq.) and ammonium acetate (5 eq.) were added. The mixture was stirred at 110 °C for 12 h. After cooling, the solution was poured into a copious amount of water. The dark precipitate was filtered. The details of purification were described for each case as follows:

2-(2-Methoxyphenyl)-1-(*p*-tolyl)-1*H*-phenanthro[9,10-*d*]imidazole (6). The product was purified by column chromatography on silica using hexanes–ethyl acetate (3/1) solution as eluent. Crystallization from chloroform–hexanes afforded a white crystalline solid (2.87 g, 86%); m.p. = 210–212 °C (chloroform–hexanes); ^{1}H NMR (500 MHz, $CDCl_3$) δ 2.41 (s, 3H), 3.57 (s, 3H), 6.75 (dd, 1H, J = 8.3 Hz, J = 0.8 Hz), 6.95–6.98 (m, 1H), 7.18–7.21 (m, 2H), 7.25–7.33 (m, 5H), 7.48–7.51 (m, 2H), 7.59–7.64 (m, 1H), 7.68–7.73 (m, 1H), 8.69–8.71 (m, 1H), 8.75–8.77 (m, 1H), 8.83–8.86 (m, 1H); ^{13}C NMR (125 MHz, $CDCl_3$) δ 21.3, 54.9, 110.5, 120.3, 120.3, 121.0, 122.8, 123.0, 123.1, 124.0, 124.7, 125.3, 126.1, 127.1, 127.4, 127.5, 128.1, 128.2, 129.1, 129.6, 131.0, 132.5, 135.6, 137.3, 138.9, 150.0, 157.7; HRMS (EI) calcd for $C_{29}H_{22}N_2O$ 414.1732, found 414.1752 [M^+].

2-(2-Hydroxyphenyl)-1-phenyl-1*H*-phenanthro[9,10-*d*]imidazole (7) and 2-(2-hydroxyphenyl)phenanthro[9,10-*d*]oxazole (8). Two products were purified by column chromatography on silica using hexanes–ethyl acetate (4/1) solution as eluent. 2-(2-Hydroxyphenyl)-1-phenyl-1*H*-phenanthro[9,10-*d*]imidazole (**7**): crystallization from chloroform–hexanes afforded a white crystalline solid (0.66 g, 42%); m.p. = 184–186 °C ($CHCl_3$–hexanes); ^{1}H NMR (500 MHz, $CDCl_3$) δ 6.49–6.53 (m, 1H), 6.75 (dd, 1H, J = 8.1 Hz, J = 1.4 Hz), 7.05 (d, 1H, J = 7.9 Hz), 7.13 (dd, 1H, J = 8.2 Hz, J = 1.1 Hz), 7.19–7.23 (m, 1H), 7.23–7.27 (m, 1H), 7.50–7.54 (m, 1H), 7.61–7.64 (m, 2H), 7.67–7.70 (m, 1H), 7.70–7.80 (m, 4H), 8.68–8.78 (m, 3H), 13.77 (s, 1H); ^{13}C NMR (125 MHz, $CDCl_3$) δ 113.0, 118.1, 120.9, 122.5, 122.6, 123.2, 124.2, 125.3, 125.6, 126.1, 126.2, 126.5, 127.0, 127.5, 128.5, 129.1, 129.5, 130.6, 130.8, 130.8, 134.2, 138.9, 148.4, 159.1; HRMS (EI) calcd for $C_{27}H_{18}N_2O$ 386.1419, found 386.1413 [M^+]; λ_{abs} [nm] (CH_3CN, $\varepsilon \times 10^{-3}$) 288 (47.6); λ_{em} [nm] (CH_3CN) 468, (MeOH) 366, (toluene) 474, (hexane) 476, (AcOH) 401.

2-(2-Hydroxyphenyl)phenanthro[9,10-*d*]oxazole (8). Crystallization from chloroform–hexanes afforded a white crystalline solid (0.1 g, 8%); m.p. = 238–240 °C ($CHCl_3$–hexanes); ^{1}H NMR (500 MHz, $CDCl_3$) δ 7.04–7.08 (m, 1H), 7.15–7.19 (m, 1H), 7.42–7.47 (m, 1H), 7.65–7.75 (m, 4H), 8.13 (dd, 1H, J = 7.8 Hz, J = 1.6 Hz), 8.26–8.30 (m, 1H), 8.43–8.47 (m, 1H), 8.66–8.72 (m, 2H), 11.43 (bs, 1H); ^{13}C NMR (125 MHz, $CDCl_3$) δ 117.4, 119.6, 120.6, 120.8, 122.8, 123.4, 123.7, 125.0, 126.4, 126.6, 126.7, 127.4, 127.5, 129.0, 129.3, 133.0, 133.3; HRMS (ESI) calcd for $C_{21}H_{14}NO_2$ 312.1019, found 312.1015 [M + H]$^+$.

2-(2-Hydroxyphenyl)-1-phenyl-1*H*-imidazo[4,5-*f*][1,10]phenanthroline (11). The product was purified by column chromatography on silica using CH_2Cl_2 → CH_2Cl_2–MeOH (40/1) solution

as eluent. Crystallization from ethyl acetate–pentane afforded a white crystalline solid (0.71 g, 61%); m.p. = 336 °C (ethyl acetate–pentane); ^{1}H NMR (500 MHz, $CDCl_3$) δ 6.52 (t, 1H, J = 7.6 Hz), 6.75 (d, 1H, J = 8.2 Hz), 7.12 (d, 1H, J = 8.2 Hz), 7.21–7.27 (m, 3H), 7.66 (d, 2H, J = 7.4 Hz), 7.72–7.84 (m, 4H), 8.92 (d, 1H, J = 8.0 Hz), 9.03 (s, 1H), 9.17 (d, 1H, J = 3.7 Hz), 13.32 (s, 1H); ^{13}C NMR (125 MHz, $CDCl_3$) δ 112.6, 118.2, 118.3, 119.5, 122.3, 122.6, 123.7, 125.8, 126.2, 128.1, 128.8, 130.4, 131.1, 131.2, 131.3, 133.1, 138.3, 144.2, 144.8, 148.2, 149.3, 149.8, 159.1; HRMS (EI) calcd for $C_{25}H_{16}N_4O$ 388.1324, found 388.1338 [M^+]; λ_{abs} [nm] (CH_3CN, $\varepsilon \times 10^{-3}$) 277 (35.1), 332 (21.8); λ_{em} [nm] (CH_3CN) 470, (CH_2Cl_2) 475.

2-(2-Methoxyphenyl)-1-phenyl-1*H*-imidazo[4,5-*f*][1,10]phenanthroline (12). The product was purified by column chromatography on silica using CH_2Cl_2–MeOH (40/1) solution as eluent. Crystallization from ethyl acetate–pentane afforded a white crystalline solid (1.01 g, 70%); m.p. = 275–276 °C (ethyl acetate–pentane); ^{1}H NMR (500 MHz, $CDCl_3$) δ 3.56 (s, 3H), 6.76 (dd, 1H, J = 8.5 Hz, J = 0.5 Hz), 6.97–7.03 (m, 1H), 7.28–7.57 (m, 9H), 7.73 (q, 1H, J = 4.3 Hz), 9.06 (dd, 1H, J = 4.3 Hz, J = 1.6 Hz), 9.14 (dd, 1H, J = 8.1 Hz, J = 1.9 Hz), 9.18 (dd, 1H, J = 4.3 Hz, J = 1.8 Hz); ^{13}C NMR (125 MHz, $CDCl_3$) δ 54.9, 110.5, 119.4, 119.8, 120.5, 122.0, 123.4, 124.1, 126.2, 128.1, 128.2, 129.3, 129.5, 130.5, 131.5, 132.3, 136.2, 137.5, 144.3, 144.8, 147.9, 148.8, 151.3, 157.4; HRMS (EI) calcd for $C_{26}H_{18}N_4O$ 402.1481, found 402.1475 [M^+].

8-(2-Hydroxyphenyl)-7-phenyl-7*H*-acenaphtho[1,2-*d*]imidazole (14). The product was purified by column chromatography on silica using hexanes–ethyl acetate (3/1 to 1/1) solution as eluent. Crystallization from $CHCl_3$–hexanes afforded an orange crystalline solid (0.76 g, 46%); m.p. = 192–194 °C ($CHCl_3$–hexanes); ^{1}H NMR (500 MHz, $CDCl_3$) δ 6.51–6.56 (m, 1H), 6.81 (dd, 1H, J = 8.1 Hz, J = 1.4 Hz), 7.03 (dd, 1H, J = 6.9 Hz, J = 0.6 Hz), 7.09–7.12 (m, 1H), 7.15–7.20 (m, 1H), 7.31–7.36 (m, 1H), 7.55–7.60 (m, 3H), 7.62–7.66 (m, 3H), 7.69–7.74 (m, 2H), 7.89–7.92 (m, 1H), 12.85 (bs, 1H); ^{13}C NMR (125 MHz, $CDCl_3$) δ 113.6, 117.8, 118.1, 119.1, 121.2, 125.9, 126.4, 126.6, 126.9, 127.0, 127.3, 127.8, 129.4, 129.5, 129.6, 129.9, 130.3, 131.6, 138.1, 138.2, 144.5, 148.3, 157.8; HRMS (EI) calcd for $C_{25}H_{16}N_2O$ 360.1263, found 360.1258 [M^+]; λ_{abs} [nm] ($CHCl_3$, $\varepsilon \times 10^{-3}$) 327 (35.0), 429 (1.4); λ_{em} [nm] ($CHCl_3$) 558.

2-(2-Nitrophenyl)-4,5-diphenyl-1-(*p*-tolyl)-1*H*-imidazole (18). Recrystallization from ethyl acetate solution afforded a yellow crystalline solid (3.41 g, 98%); m.p. = 184 °C (ethyl acetate); ^{1}H NMR (400 MHz, $CDCl_3$) δ 2.23 (s, 3H), 6.82 (d, 2H, J = 8.4 Hz), 6.93 (d, 2H, J = 8.0 Hz), 7.16–7.30 (m, 8H), 7.47–7.52 (m, 1H), 7.55–7.69 (m, 4H), 7.89–7.93 (m, 1H); ^{13}C NMR (100 MHz, $CDCl_3$) δ 21.3, 124.7, 126.9, 127.6, 127.9, 128.3, 128.4, 128.7, 129.8, 130.2, 130.5, 130.9, 131.2, 133.1, 133.2, 133.6, 134.5, 138.3, 138.8, 143.5, 149.1, 182.4; HRMS (EI) calcd for $C_{28}H_{21}N_3O_2$ 431.1634, found 431.1619 [M^+]; λ_{abs} [nm] (CH_3CN, $\varepsilon \times 10^{-3}$) 268 (21).

2-(2-*N*,*N*-Dimethylaniline)-4,5-diphenyl-1-(*p*-tolyl)-1*H*-imidazole (22). The product was purified by column chromatography on silica using hexanes–ethyl acetate (3/1) solution as eluent. Crystallization from ethyl acetate–hexanes afforded a white crystalline solid (2.12 g, 82%); m.p. = 168–169 °C (ethyl acetate–hexanes); ^{1}H NMR (500 MHz, $CDCl_3$) δ 2.19 (s, 3H), 2.31 (s, 6H), 6.65 (dd, 1H, J = 8.2 Hz, J = 1.0 Hz), 6.68–6.69 (m, 2H), 6.81–6.85 (m, 2H), 6.93–6.97 (m, 1H), 7.13–7.26 (m, 9H), 7.58–7.63 (m, 3H); ^{13}C NMR (125 MHz, $CDCl_3$) δ 21.0, 42.1, 117.1, 120.6, 123.6, 126.3, 126.5, 127.3, 127.7, 128.0, 128.3, 128.3, 129.3, 129.8, 131.1, 131.2, 132.8, 134.6, 134.8, 136.7, 138.0, 147.6, 151.7; HRMS (EI) calcd for $C_{30}H_{27}N_3$ 429.2205, found 429.2216 [M^+].

2-(2-Nitrophenyl)-1-(*p*-tolyl)-1*H*-phenanthro[9,10-*d*]imidazole (23). The product was purified by column chromatography on silica using hexanes–ethyl acetate (3/2 to 1/1) solution as eluent. Crystallization from ethyl acetate afforded an orange crystalline solid (1.56 g, 91%); m.p. = 262–263 °C (ethyl acetate); ^{1}H NMR (500 MHz, $CDCl_3$) δ 2.42 (s, 3H), 7.21–7.32 (m, 6H), 7.50–7.55 (m, 2H), 7.60–7.66 (m, 3H), 7.68–7.73 (m, 1H), 8.01 (d, 1H, J = 8.0 Hz), 8.71 (d, 1H, J = 8.4 Hz), 8.74–8.79 (m, 2H); ^{13}C NMR (125 MHz, $CDCl_3$) δ 21.3, 120.9, 122.7, 122.9, 123.1, 124.1, 124.6, 125.1, 125.6, 126.3, 126.7, 127.2, 127.3, 127.7, 128.3, 128.3, 129.3, 130.3, 130.4, 132.9, 133.5, 134.5, 137.5, 139.7, 147.7, 148.9; HRMS (EI) calcd for $C_{28}H_{19}N_3O_2$ 429.1477, found 429.1488 [M^+].

2-(1*H*-Indol-7-yl)-1-(*p*-tolyl)-1*H*-phenanthro[9,10-*d*]imidazole (27). Following the general procedure for **1**, the product was purified by column chromatography on silica using hexanes–ethyl acetate (7/1) solution as eluent. Crystallization from ethyl acetate–hexanes afforded a white crystalline solid (40 mg, 10%) m.p. = 105–106 °C (ethyl acetate–hexanes); ^{1}H NMR (500 MHz, $CDCl_3$) δ 2.60 (s, 3H), 6.61–6.64 (m, 1H), 6.73 (dd, 1H, J = 7.6 Hz, J = 0.6 Hz), 6.81 (t, 1H, J = 7.7 Hz), 7.18 (dd, 1H, J = 8.4 Hz, J = 1.0 Hz), 7.25–7.30 (m, 1H), 7.45–7.53 (m, 6H), 7.62 (d, 1H, J = 7.8 Hz), 7.64–7.69 (m, 1H), 7.75–7.80 (m, 1H), 8.71 (d, 1H, J = 8.4 Hz), 8.77 (d, 1H, J = 8.3 Hz), 8.89 (dd, 1H, J = 7.9 Hz, J = 1.1 Hz), 11.50 (bs, 1H); ^{13}C NMR (125 MHz, $CDCl_3$) δ 21.6, 102.4, 118.6, 120.2, 121.0, 122.0, 122.5, 123.1, 123.2, 124.1, 124.9, 125.6, 126.4, 127.2, 127.7, 128.3, 128.8, 128.8, 129.3, 131.2, 135.0, 136.7, 140.4, 148.8; HRMS (EI) calcd for $C_{30}H_{21}N_3$ 423.1735, found 423.1746 [M^+]; λ_{em} [nm] (CH_3CN) 379, 397.

2-(2-Methoxyphenyl)phenanthro[9,10-*d*]oxazole (9). CH_3I (46 mg, 0.32 mmol) was added dropwise to a suspension of **8** (50 mg, 0.16 mmol) and K_2CO_3 (45 mg, 0.32 mmol) in acetone (40 ml). The reaction was refluxed overnight. After cooling, the organic layer was distilled off and the product was purified by column chromatography using hexanes–ethyl acetate (2/1) solution as eluent. Crystallization from chloroform–hexanes afforded a white crystalline solid (46 mg, 88%); ^{1}H NMR (500 MHz, $CDCl_3$) δ 4.06 (s, 3H), 7.08–7.17 (m, 2H), 7.48–7.53 (m, 1H), 7.64–7.77 (m, 4H), 8.26 (ddd, 1H, J = 7.8 Hz, J = 1.8 Hz, J = 0.3 Hz), 8.31–8.35 (m, 1H), 8.66–8.76 (m, 3H); ^{13}C NMR (125 MHz, $CDCl_3$) δ 56.2, 112.2, 116.7, 120.8, 121.0, 121.1, 123.1, 123.3, 123.7, 126.0, 126.3, 127.1, 127.3, 128.8, 129.2, 131.1, 132.3, 135.3, 158.2, 160.8; HRMS (EI) calcd for $C_{22}H_{15}NO_2$ 325.1103, found 325.1095 [M^+].

8-(2-Methoxyphenyl)-7-phenyl-7*H*-acenaphtho[1,2-*d*]imidazole (15). CH_3I (46 mg, 0.32 mmol) was added dropwise to a

suspension of **14** (59 mg, 0.16 mmol) and K_2CO_3 (45 mg, 0.32 mmol) in acetone (40 ml). The reaction was refluxed overnight. After cooling, the organic layer was distilled off and the product was purified by crystallization from chloroform–hexanes, affording an orange crystalline solid (61 mg, 99%); m.p. = 154–156 °C ($CHCl_3$–hexanes); ^{1}H NMR (500 MHz, $CDCl_3$) δ 3.31 (s, 3H), 6.73 (d, 1H, J = 8.0 Hz), 7.02–7.04 (m, 1H), 7.32–7.44 (m, 8H), 7.52–7.56 (m, 1H), 7.66–7.72 (m, 3H), 7.92 (d, 1H, J = 6.6 Hz); ^{13}C NMR (125 MHz, $CDCl_3$) δ 54.6, 110.8, 118.8, 120.4, 120.5, 120.8, 124.4, 126.3, 126.8, 126.9, 127.3, 127.7, 127.8, 129.0, 129.5, 130.8, 130.9, 131.5, 132.1, 137.1, 138.4, 148.0, 148.6, 156.8; HRMS (EI) calcd for $C_{26}H_{18}N_2O$ 374.1419, found 374.1411 [M^+].

2-(2-Aniline)-4,5-diphenyl-1-(*p*-tolyl)-1*H*-imidazole (19). Compound **18** (1.5 g, 3.48 mmol) was dissolved in 150 ml of ethanol–ethyl acetate (2/1) and reduced with hydrogen (1 atm) on 10% Pd–C (0.22 g) as a catalyst. The catalyst was filtered off and the filtrate was evaporated under reduced pressure. Recrystallization from ethyl acetate solution afforded a yellow crystalline solid (1.33 g, 95%); m.p. = 202–203 °C (ethyl acetate); ^{1}H NMR (500 MHz, DMSO) δ 2.20 (s, 3H), 6.06 (s, 2H), 6.21–6.25 (m, 1H), 6.63 (dd, 1H, J = 7.8 Hz, J = 1.5 Hz), 6.73 (dd, 1H, J = 8.2 Hz, J = 1.1 Hz), 6.91–6.95 (m, 1H), 7.01–7.06 (m, 4H), 7.12–7.17 (m, 1H), 7.19–7.24 (m, 4H), 7.26–7.30 (m, 3H), 7.42–7.46 (m, 2H); ^{13}C NMR (125 MHz, DMSO) δ 21.0, 113.1, 115.2, 116.0, 126.7, 126.8, 128.6, 128.7, 128.8, 128.9, 129.5, 129.9, 130.0, 130.5, 131.1, 131.6, 134.7, 134.8, 136.2, 138.1, 145.7, 148.2; HRMS (EI) calcd for $C_{28}H_{23}N_3$ 401.1892, found 401.1896 [M^+]; λ_{abs} [nm] ($CHCl_3$, $\varepsilon \times 10^{-3}$) 282 (17); λ_{em} [nm] (CH_2Cl_2) 393, (CH_3CN) 401.

***N*-{2-[4,5-Diphenyl-1-(*p*-tolyl)-1*H*-imidazol-2-yl]phenyl}-4-methylbenzenesulfonamide (20).** *p*-Toluenesulfonyl chloride (129 mg, 0.675 mmol) was added to a solution of **19** (201 mg, 0.5 mmol) in pyridine (3 ml), and the mixture was heated at reflux for 16 h. After cooling, the solution was poured into a copious amount of water. The light brown precipitate was filtered and washed with water. The product was purified by column chromatography on silica using hexanes–ethyl acetate (4/1) solution as eluent. Recrystallization from ethyl acetate–pentane solution afforded a white crystalline solid (272 mg, 98%); m.p. = 258 °C (ethyl acetate–pentane); ^{1}H NMR (500 MHz, $CDCl_3$) δ 2.28 (s, 3H), 2.34 (s, 3H), 6.27 (bs, 2H), 6.53 (d, 1H, J = 7.4 Hz), 6.73 (t, 1H, J = 7.4 Hz), 6.93 (d, 2H, J = 8.2 Hz), 7.05 (d, 2H, J = 6.8 Hz), 7.14 (d, 2H, J = 8.2 Hz), 7.18–7.23 (m, 1H), 7.23–7.33 (m, 6H), 7.53 (d, 2H, J = 8.0 Hz), 7.61 (d, 2H, J = 7.4 Hz), 7.76 (bs, 1H), 11.76 (bs, 1H); ^{13}C NMR (125 MHz, $CDCl_3$) δ 21.1, 21.4, 120.1, 123.9, 124.6, 126.9, 127.1, 127.4, 127.7, 128.5, 128.8, 129.1, 129.7, 130.1, 130.5, 131.1, 133.4, 133.7, 136.4, 137.2, 138.5, 143.0, 143.1; HRMS (EI) calcd for $C_{35}H_{29}N_3O_2S$ 555.1980, found 555.1959 [M^+]; λ_{abs} [nm] ($CHCl_3$, $\varepsilon \times 10^{-3}$) 289 (20.4), 276 (20); λ_{em} [nm] (CH_2Cl_2) 475, (CH_3CN) 429.

2-(1-(*p*-Tolyl)-1*H*-phenanthro[9,10-*d*]imidazol-2-yl)aniline (24). Compound **23** (0.54 g, 1.36 mmol) was dissolved in 200 ml ethyl acetate and reduced with hydrogen (1 atm) on 10% Pd–C (0.08 g) as a catalyst. The catalyst was filtered off and the filtrate was evaporated under reduced pressure. Crystallization from ethyl acetate solution afforded a white crystalline solid (0.50 g, 99%); m.p. = 202–203 °C (ethyl acetate); ^{1}H NMR (500 MHz, $CDCl_3$) δ 2.49 (s, 3H), 5.26 (s, 2H), 6.41–6.46 (m, 1H), 6.76 (dd, 1H, J = 8.0 Hz, J = 0.7 Hz), 6.87 (dd, 1H, J = 7.9 Hz, J = 1.3 Hz), 7.03–7.08 (m, 1H), 7.23–7.38 (m, 6H), 7.47–7.52 (m, 1H), 7.61–7.66 (m, 1H), 7.69–7.74 (m, 1H), 8.70 (d, 1H, J = 8.4 Hz), 8.76 (d, 1H, J = 8.4 Hz), 8.80 (dd, 1H, J = 7.9 Hz, J = 1.0 Hz); ^{13}C NMR (125 MHz, $CDCl_3$) δ 21.4, 113.9, 116.3, 116.7, 121.1, 122.6, 123.1(2), 124.0, 124.8, 125.5, 126.3, 127.0, 127.2, 127.2, 128.2, 128.7, 129.1, 129.8, 130.3, 130.6, 136.0, 136.6, 139.6, 147.3, 149.5; HRMS (EI) calcd for $C_{28}H_{21}N_3$ 399.1735, found 399.1727 [M^+].

4-Methyl-*N*-(2-(1-(*p*-tolyl)-1*H*-phenanthro[9,10-*d*]imidazol-2-yl)phenyl)benzenesulfonamide (25). *p*-Toluenesulfonyl chloride (72 mg, 0.38 mmol) was added to a solution of **24** (120 mg, 0.25 mmol) in pyridine (5 ml), and the mixture was heated at reflux for 2 h. After cooling, the solution was poured into a copious amount of water. The white precipitate was filtered and washed with water. The product was purified by column chromatography on silica using dichloromethane as eluent. Recrystallization from dichloromethane–pentane solution afforded a white crystalline solid (154 mg, 93%); m.p. = 195–196 °C (dichloromethane–pentane); ^{1}H NMR (500 MHz, $CDCl_3$) δ 2.03 (s, 3H), 2.51 (s, 3H), 6.70–6.81 (m, 6H), 7.08 (dd, 1H, J = 8.2 Hz, J = 0.7 Hz), 7.23–7.31 (m, 4H), 7.36 (d, 2H, J = 8.4 Hz), 7.53–7.57 (m, 1H), 7.69–7.74 (m, 1H), 7.79–7.83 (m, 2H), 8.73 (d, 1H, J = 8.4 Hz), 8.80 (d, 1H, J = 8.4 Hz), 8.84 (dd, 1H, J = 7.9 Hz, J = 0.8 Hz), 11.66 (s, 1H); ^{13}C NMR (125 MHz, $CDCl_3$) δ 21.1, 21.4, 120.2, 121.0, 122.6, 122.7, 123.1, 123.9, 124.2, 124.7, 125.4, 126.2, 126.4(2), 127.0, 127.2, 127.9, 128.2, 128.4, 128.8, 129.0, 129.6, 129.7, 130.8, 135.3, 136.1, 136.9(2), 140.1, 143.0, 146.8; HRMS (EI) calcd for $C_{35}H_{27}N_3O_2S$ 553.1824, found 553.1835 [M^+].

Linear optical properties

The solvents used were spectroscopic grade toluene, dichloromethane and methanol (C. Erba). Absorption spectra were recorded with a Perkin-Elmer Lambda 650 spectrophotometer and the emission spectra, corrected for the photomultiplier response if not otherwise stated, were detected by an Edinburgh FSP920 fluorometer equipped with a R928P Hamamatsu photomultiplier. Luminescence quantum yields of the samples, ϕ_s, were evaluated against a standard with known emission quantum yield, ϕ_r, by comparing areas under the corrected luminescence spectra using the equation: $\phi_s/\phi_r = A_r n^2_s (\text{area})_s / A_s n^2_r (\text{area})_r$, where A is the absorbance, n is the refractive index of the solvent employed and s and r stand for sample and reference, respectively. The standard used was air-equilibrated quinine sulphate in 1 N H_2SO_4 with an emission quantum yield $\phi_{fl} = 0.546$.[45] Keto and enol quantum yields were obtained by spectral deconvolution by Microcal™ Origin® 6.1.

Estimated errors are 10% on molar extinction coefficients and quantum yields and 2 nm on emission and absorption maxima. The working temperature, if not otherwise specified, is 295 ± 2 K.

Non-linear optical properties

Two-photon absorption (TPA) measurements were conducted by investigating the two-photon excited fluorescence (TPEF) of the fluorophores in solution at room temperature on air-equilibrated solutions (10^{-4} M), according to the experimental protocol established by Xu and Webb.[46] This protocol avoids contributions from excited-state absorption that are known to result in overestimated TPA cross-sections. To span the 700–980 nm range, a Nd:YLF-pumped Ti:sapphire oscillator was used generating 150 fs pulses at a 76 MHz rate. The excitation was focused onto the cuvette through a microscope objective (10×, NA 0.25). The fluorescence was detected in epifluorescence mode *via* a dichroic mirror (Chroma 675dcxru) and a barrier filter (Chroma e650sp-2p) by a compact CCD spectrometer module BWTek BTC112E. Total fluorescence intensities were obtained by integrating the corrected emission spectra measured by this spectrometer. TPA cross-sections (σ_2) were determined from the two-photon excited fluorescence (TPEF) cross-sections ($\sigma_2\Phi$) and the fluorescence emission quantum yield (Φ). TPEF cross-sections were measured relative to fluorescein in 0.01 M aqueous NaOH for 715–980 nm,[47] and the appropriate solvent-related refractive index corrections.[48] Data points between 700 and 715 nm were corrected according to ref. 49. The quadratic dependence of the fluorescence intensity on the excitation power was checked for each sample and all wavelengths, indicating that the measurements were carried out in intensity regimes where saturation or photodegradation did not occur.

Acknowledgements

Financial support for our work from the Foundation for Polish Science (Grant number TEAM/2009-4/3) is gratefully acknowledged. The research leading to these results has received partial funding from the European Community's Seventh Framework Programme under the TOPBIO project-grant agreement no. 264362. E. N. thanks Caltech SURF Program and Hugh F. and Andy Lou Colvin.

Notes and references

1 (*a*) M. R. Grimmet, *Comprehensive Heterocyclic Chemistry*, ed. A. R. Katritzky and C. W. Rees, Pergamon, New York, 1984, vol. 5, p. 457; (*b*) M. R. Grimmet, *Comprehensive Heterocyclic Chemistry II*, ed. A. R. Katritzky, C. W. Rees and E. F. V. Scriven, Pergamon, New York, 1996, vol. 3, p. 77; (*c*) P. Molina, A. Tárraga and F. Otón, *Org. Biomol. Chem.*, 2012, **10**, 1711.
2 H. Debus, *Liebigs Ann. Chem.*, 1858, **107**, 199.
3 B. Radziszewski, *Chem. Ber.*, 1882, **15**, 1493.
4 (*a*) T. Hayashi and K. Maeda, *Bull. Chem. Soc. Jpn.*, 1962, **35**, 2057; (*b*) T. Hayashi, K. Maeda, S. Shida and K. Nakada, *J. Chem. Phys.*, 1960, **32**, 1568; (*c*) H. Zimmerman, H. Baumgärtel and F. Bakke, *Angew. Chem.*, 1961, **73**, 808; (*d*) S. M. Blinder, M. J. Peller, N. W. Lord, K. C. Aamodt and N. S. Ivanchukov, *J. Chem. Phys.*, 1962, **36**, 540; (*e*) H. Igarashi, T. Igarashi, M. Sagawa, T. Mori, Y. Kotani, Y. Muroya, Y. Katsumura and T. Yamashita, *J. Photopolym. Sci. Technol.*, 2007, **20**, 757.
5 (*a*) E. H. White and M. J. C. Harding, *Photochem. Photobiol.*, 1965, **4**, 1129; (*b*) G. E. Philbrook, M. A. Maxwell, R. Taylor and G. Totter, *Photochem. Photobiol.*, 1965, **4**, 1175.
6 (*a*) S. Park, O. H. Kwon, S. Kim, S. Park, M. G. Choi, M. Cha, S. Y. Park and D. J. Jang, *J. Am. Chem. Soc.*, 2005, **127**, 10070; (*b*) S. Park, J. E. Kwon, S.-H. Kim, J. Seo, K. Chung, S.-Y. Park, D.-J. Jang, B. M. Medina, J. Gierschner and S.-Y. Park, *J. Am. Chem. Soc.*, 2009, **131**, 14043.
7 (*a*) J. E. Kwon and S.-Y. Park, *Adv. Mater.*, 2011, **23**, 3615–3642; (*b*) C. Fang, N. N. Frontiera, R. Tran and R. A. Mathies, *Nature*, 2009, **462**, 200–204; (*c*) A. Douhal, F. Lahmani and A. H. Zewail, *Chem. Phys.*, 1996, **207**, 477.
8 (*a*) J. S. Kim and D. T. Quang, *Chem. Rev.*, 2007, **107**, 3780; (*b*) B. Wang, V. Eric and E. V. Anslyn, *Chemosensors: Principles, Strategies, and Applications*, Wiley, 2011, pp. 253–273; (*c*) A. D. Roshal, A. V. Grigorovich, A. O. Doroshenko and V. G. Pivovarenko, *J. Phys. Chem. A*, 1998, **102**, 5907; (*d*) S. M. Landge, K. Tkatchouk, D. Benitez, D. A. Lanfranchi, M. Elhabiri, W. A. Goddard III and I. Aprahamian, *J. Am. Chem. Soc.*, 2011, **133**, 9812; (*e*) D. A. Svechkarev, G. V. Karpushina, L. L. Lukatskaya and A. O. Doroshenko, *Cent. Eur. J. Chem.*, 2008, **6**, 443–449.
9 (*a*) A. Mordziński, A. Grabowska, W. Kuhnle and A. Krowczyński, *Chem. Phys. Lett.*, 1983, **101**, 291; (*b*) W. Frey, F. Laermer and T. Elsaesser, *J. Phys. Chem.*, 1991, **95**, 10391; (*c*) K. Das, N. Sarkar, D. Majumda and K. Bhattacharyya, *Chem. Phys. Lett.*, 1992, **198**, 443; (*d*) M. Fores, M. Duran, M. Sola and L. Adamowicz, *J. Phys. Chem. A*, 1999, **103**, 4413; (*e*) H. Wang, H. Zhang, O. K. Abou-Zied, C. Yu, F. E. Romesberg and M. Glasbeek, *Chem. Phys. Lett.*, 2003, **367**, 599; (*f*) M. Rini, J. Dreyer, E. T. J. Nibbering and T. Elsaesser, *Chem. Phys. Lett.*, 2003, **374**, 13; (*g*) W. Chen, E. B. Twum, L. Li, B. D. Wright, P. L. Rinaldi and Y. Pang, *J. Org. Chem.*, 2012, **77**, 285–290; (*h*) Y. Pang and W. Chen, in *Hydrogen Bonding and Transfer in the Excited State*, ed. K.-L. Han and G.-J. Zhao, Wiley, Chichester, 2011, vol. 2, pp. 747–760.
10 (*a*) D. McMorrow and M. Kasha, *J. Phys. Chem.*, 1984, **88**, 2235; (*b*) A. J. G. Strandjord, D. E. Smith and P. F. Barbara, *J. Phys. Chem.*, 1985, **89**, 2362; (*c*) P.-T. Chou, Y.-C. Chen, W.-S. Yu and Y.-M. Chen, *Chem. Phys. Lett.*, 2001, **340**, 89.
11 (*a*) M. L. Martinez, W. C. Cooper and P.-T. Chou, *Chem. Phys. Lett.*, 1992, **193**, 151; (*b*) P.-T. Chou, Y.-C. Chen, W.-S. Yu, Y.-H. Chou, C.-Y. Wei and Y.-M. Cheng, *J. Phys. Chem. A*, 2001, **105**, 1731–1740; (*c*) K.-Y. Chen, C.-C. Hsieh, Y.-M. Cheng, C.-H. Lai and P.-T. Chou, *Chem. Commun.*, 2006, 4395; (*d*) J. Piechowska and D. T. Gryko, *J. Org. Chem.*, 2011, **76**, 10220.
12 (*a*) A. Douhal, F. Amat-Guerri and A. U. Acuña, *J. Phys. Chem.*, 1995, **99**, 76; (*b*) A. Douhal, F. Amat-Guerri and A. U. Acuña, *Angew. Chem., Int. Ed. Engl.*, 1997, **36**, 1514; (*c*) A. Douhal, *Ber. Bunsen-Ges. Phys. Chem.*, 1998, **102**, 448; (*d*) H. Shono, T. Ohkava, H. Tomoda, T. Mutai and K. Araki, *ACS Appl. Mater. Interfaces*, 2011, **3**, 654; (*e*) T. Mutai, H. Tomoda, T. Ohkawa, Y. Yabe and K. Araki, *Angew. Chem., Int. Ed.*, 2008, **47**, 9522; (*f*) A. J. Stasyuk, M. Banasiewicz, M. K. Cyrański and D. T. Gryko, *J. Org. Chem.*, 2012, **77**, 5552–5558.
13 (*a*) P. T. Chou, D. McMorrow, T. J. Aartsma and M. Kasha, *J. Phys. Chem.*, 1984, **88**, 4596; (*b*) A. V. Acuna, F. Amat-Guerri, J. Catalán, A. Costella, J. Figuera and J. Munoz, *J. Phys. Chem. Lett.*, 1986, **132**, 576; (*c*) K. I. Sakai, T. Tsuzuki, Y. Itoh, M. Ichikawa and Y. Taniguchi, *Appl. Phys. Lett.*, 2005, **86**, 081103.
14 (*a*) S. Kim and S.-Y. Park, *Adv. Mater.*, 2003, **15**, 1341; (*b*) S. Kim, S.-Y. Park, I. Tashida, H. Kawai and T. Nagamura, *J. Phys. Chem. B*, 2002, **106**, 9291.
15 J. Catalán, J. C. del Valle, R. M. Claramunt, D. Sanz and J. Dotor, *J. Lumin.*, 1996, **68**, 165.
16 F. Parsapour and D. F. Kelley, *J. Phys. Chem.*, 1996, **100**, 2791.
17 A. Sytnik and M. Kasha, *Proc. Natl. Acad. Sci. U. S. A.*, 1994, **91**, 8627.
18 S. Kim, J. Seo, H. K. Jung, J. J. Kim and S.-Y. Park, *Adv. Mater.*, 2005, **17**, 2077.
19 (*a*) B. Liu, H. Wang, T. Wang, Y. Bao, F. Du, J. Tian, Q. Li and R. Bai, *Chem. Commun.*, 2012, **48**, 2867; (*b*) J. Zhao, S. Ji, Y. Chen, H. Guo and P. Yang, *Phys. Chem. Chem. Phys.*, 2012, **14**, 8803.
20 (*a*) K. Ding, S. J. Courtney, A. J. Strandjord, S. Flom, D. Friedrich and P. F. Barbara, *J. Phys. Chem.*, 1983, **87**, 1184–1188; (*b*) S. R. Grando, C. M. Pessoa, M. R. Gallas, T. M. H. Costa, F. S. Rodembusch and E. V. Benvenutti, *Langmuir*, 2009, **25**, 13219; (*c*) D. Yao, S. Zhao, J. Guo, Z. Zhang, H. Zhang, Y. Liu and Y. Wang, *J. Mater. Chem.*, 2011, **21**, 3568.

21 R. G. Harvey, *Polycyclic Aromatic Compounds*, Wiley, New York, 1997.
22 (*a*) A. H. Cook and D. H. Jones, *J. Chem. Soc.*, 1941, 278–282; (*b*) A. I. Shienok, L. S. Koltsova, N. L. Zaichenko and V. S. Marevtsev, *Russ. Chem. Bull.*, 2002, **51**, 2050.
23 M. F. Rode and A. L. Sobolewski, *J. Phys. Chem. A*, 2010, **114**, 11879.
24 A. O. Doroshenko, E. A. Posokhov, V. M. Shershukov, V. G. Mitina and O. A. Ponomarev, *Chem. Heterocycl. Compd.*, 1995, **31**, 492.
25 F. R. Japp and E. Wilcock, *J. Chem. Soc. Trans.*, 1880, **37**, 661–672.
26 (*a*) J. D. Spence and T. D. Lash, *J. Org. Chem.*, 2000, **65**, 1530–1539; (*b*) J. P. Lewtak and D. T. Gryko, *Chem. Commun.*, 2012, DOI: 10.1039/c2cc31279d.
27 E. K. Dora, B. Dash and C. S. Panda, *J. Indian Chem. Soc.*, 1979, **56**, 620–624.
28 (*a*) O. Tsuge and M. Tashiro, *Bull. Chem. Soc. Jpn.*, 1963, **36**, 970–975; (*b*) D. M. White, *J. Org. Chem.*, 1970, **35**, 2452.
29 F. C. Krebs and M. Jørgensen, *J. Org. Chem.*, 2001, **66**, 6169–6173.
30 (*a*) O. K. Abou-Zied, R. Jimenez, E. H. Z. Thompson, D. P. Millar and F. E. Romeberg, *J. Phys. Chem. A*, 2002, **106**, 3665; (*b*) S. R. Vazquesz, M. C. R. Rodriguez, M. Mosquera and F. Rodriguez-Prieto, *J. Phys. Chem. A*, 2008, **112**, 376.
31 T. Iijima, A. Momotake, Y. Shinohara, T. Sato, Y. Nishimura and T. Arai, *J. Phys. Chem. A*, 2010, **114**, 1603.
32 A. O. Eseola, W. Li, W.-H. Sun, M. Zhang, L. Xiao and J. A. O. Woods, *Dyes Pigm.*, 2011, **88**, 262–273.
33 (*a*) A. Mahajan, R. K. Aulakh, R. K. Bedi, S. Kumar, S. Kumar and D. K. Aswal, *Synth. Met.*, 2012, **162**, 58–63; (*b*) A. O. Eseola, O. Adepitan, H. Görls and W. Plass, *New J. Chem.*, 2012, **36**, 891.
34 (*a*) J. Jayabharathi, V. Thanikachalam, N. Srinivasan and K. Saravanan, *J. Fluoresc.*, 2011, **21**, 595; (*b*) T. F. Markle, I. J. Rhile, A. G. DiPasquale and J. M. Mayer, *Proc. Natl. Acad. Sci. U. S. A.*, 2008, **105**, 8185.
35 S. Park, J. E. Kwon and S. Y. Park, *Phys. Chem. Chem. Phys.*, 2012, **14**, 8878–8884.
36 (*a*) J. Jayabharathi, V. Thanikachalam, M. V. Perumal and N. Srinivasan, *J. Fluoresc.*, 2012, **22**, 409–417; (*b*) J. Jayabharathi, V. Thanikachalam and M. V. Perumal, *Spectrochim. Acta, Part A*, 2012, **92**, 113–121; (*c*) Y. Yuan, D. Li, X. Zhang, X. Zhao, Y. Liu, J. Zhang and Y. Wang, *New J. Chem.*, 2011, **35**, 1534–1540.
37 (*a*) D. T. Gryko, J. Piechowska and M. Gałęzowski, *J. Org. Chem.*, 2010, **75**, 1297; (*b*) I. Deperasińska, D. T. Gryko, E. Karpiuk, B. Kozankiewicz, A. Makarewicz and J. Piechowska, *J. Phys. Chem. A*, 2012, **116**, 2109–2116.
38 K. Buttke, H. Baumgärtel, H.-J. Niclas and M. Schneider, *J. Prakt. Chem.*, 1997, **339**, 721–728.
39 C.-C. Hsieh, C.-M. Jiang and P.-T. Chou, *Acc. Chem. Res.*, 2010, **43**, 1364–1374.
40 (*a*) C. J. Fahrni, M. M. Henary and D. G. VanDerveer, *J. Phys. Chem. A*, 2002, **106**, 7655; (*b*) M. M. Henary, Y. Wu, J. Cody, S. Sumaleksmy, J. Li, S. Mandal and C. J. Fahrni, *J. Org. Chem.*, 2007, **72**, 4784.
41 J. C. Penedo, M. Mosquera and F. Rodriguez-Prieto, *J. Phys. Chem. A*, 2000, **104**, 7429–7441.
42 Y. M. Cheng, S. C. Pu, C. J. Hsu, C. H. Lai and P. T. Chou, *ChemPhysChem*, 2006, **7**, 1372–1381.
43 M. M. Henary, Y. Wu and C. J. Fahrni, *J. Phys. Chem. A*, 2002, **106**, 5210–5220.
44 W. Paw and R. Eisenberg, *Inorg. Chem.*, 1997, **36**, 2287.
45 D. F. Eaton, *Pure Appl. Chem.*, 1988, **60**, 1107–1114.
46 C. Xu and W. W. Webb, *J. Opt. Soc. Am. B*, 1996, **13**, 481–491.
47 M. A. Albota, C. Xu and W. W. Webb, *Appl. Opt.*, 1998, **37**, 7352–7356.
48 M. H. V. Werts, N. Nerambourg, D. Pélégry, Y. Le Grand and M. Blanchard-Desce, *Photochem. Photobiol. Sci.*, 2005, **4**, 531–538.
49 C. Katan, S. Tretiak, M. H. V. Werts, A. J. Bain, R. J. Marsh, N. Leonczek, N. Nicolaou, E. Badaeva, O. Mongin and M. Blanchard-Desce, *J. Phys. Chem. B*, 2007, **111**, 9468–9483.